IN 163

AMRC-R-12

TRANSIENT CURRENT ESTIMATES FOR FINITE LENGTH SURFACE CABLES

Monti R. Wilson

May 1973

Prepared for

Harry Diamond Laboratories
Connecticut and Van Ness Street, N. W.
Washington, D. C. 20438

Under Contract

DAAG39-73-C-0049

MISSION RESEARCH CORPORATION
Post Office Box 8693
Albuquerque, New Mexico 87108

With Offices in the Apollo Building
5601 Domingo Road N. E.

Abstract

A finite length insulated wire lying at the earth-air interface is modeled using a transmission line approach. Transient response to a double exponential incident pulse with 10 ns rise time is obtained for various incident polarizations, cable lengths, soil conductivities and termination impedances. Characterizing all cases, the induced current pulses peak at ~(3-20) amps/kv with rise time ~(.1-.2) μsec. A simple bare wire surface cable model current estimate is shown to be in good agreement with results from a more sophisticated model of a wire near the ground plane.

TABLE OF CONTENTS

Section		Page
1	Introduction	1
2	The Surface Cable Transmission Line Model	2
3	Numerical Results	8
4	Conclusions	9
5	References	22
APPENDIX		
A	Transfer Function for End-On Illumination	A-1
B	Natural Mode Buried Cable Model	B-1A
C	Comparison of A Bare Wire Surface Cable Estimate and Results from a Greens Function Treatment of a Wire Near a Finitely conducting Ground Plane	C-1

LIST OF ILLUSTRATIONS

Figure		Page
1	Cross Section of Surface Cable	2
2	Surface Cable Transmission Line	2
3	Sphere Termination	7
4-14	Cable Current Versus Time	11-21
Appendix A		
A-1	Surface Wave Geometry	A-1
Appendix B		
B-1	Incremental Section of Transmission Line	B-3
B-2	Coaxial Transmission Line Section	B-5
B-3	Cable Geometry	B-7
B-4	Bare Wire	B-13
B-5	Bare Wire Transmission Line Section	B-15
B-6	Real Parts of Propagation Constant Versus Frequency	B-27
B-7	Imaginary Part of Propagation Constant Versus Frequency	B-27
B-8	Real Part of Characteristic Impedance Versus Frequency	B-28
B-9	Imaginary Part of Characteristic Impedance Versus Frequency	B-28

LIST OF ILLUSTRATIONS (Continued)

Appendix B (continued)		Page
B-10	Real Part of Longitudinal Impedance Versus Frequency	B-29
B-11	Imaginary Part of Longitudinal Impedance Versus Frequency	B-29
B-12	Real Part of Transverse Admittance Versus Frequency	B-30
B-13	Imaginary Part of Transverse Admittance Versus Frequency	B-30
B-14	Real Part of Propagation Constant Versus Frequency	B-31
B-15	Imaginary Part of Propagation Constant Versus Frequency	B-31
B-16	Real Part of Characteristic Impedance Versus Frequency	B-32
B-17	Imaginary Part of Characteristic Impedance Versus Frequency	B-32
B-18	Real Part of Longitudinal Impedance Versus Frequency	B-33
B-19	Imaginary Part of Longitudinal Impedance Versus Frequency	B-33
B-20	Real Part of Transverse Admittance Versus Frequency	B-34
B-21	Imaginary Part of Transverse Admittance Versus Frequency	B-34
B-22	Real Part of Propagation Constant Versus Frequency	B-35
B-23	Imaginary Part of Propagation Constant Versus Frequency	B-35
B-24	Real Part of Characteristic Impedance Versus Frequency	B-36
B-25	Imaginary Part of Characteristic Impedance Versus Frequency	B-36

LIST OF ILLUSTRATIONS (Continued)

Appendix B (continued)		Page
B-26	Real Part of Longitudinal Impedance Versus Frequency	B-37
B-27	Imaginary Part of Longitudinal Impedance Versus Frequency	B-37
B-28	Real Part of Transverse Admittance Versus Frequency	B-38
B-29	Imaginary Part of Transverse Admittance Versus Frequency	B-38
A-1	Bare Wire TM Waveguide Equivalent Circuit	B-43

Appendix C

C-1(a)	Wire Near Ground, but with $y_o >> a$	C-1
C-1(b)	Surface cable; treatment analogous to that of reference 1	C-1
C-2	Comparison of Surface Cable Estimate and Bombardt	C-4

TRANSIENT CURRENT ESTIMATES FOR FINITE LENGTH SURFACE CABLES

1. INTRODUCTION

In a previous note [1] we reexamined an approximate theory applicable to studying the EMP response of surface cables interconnecting equipment components of mobile defense systems. Explicit finite difference calculations [1] of the step pulse response of an infinite (no axial dependence) surface cable revealed that a reasonable estimate of the surface cable transmission line impedance could be obtained from the impedance of a cable fully buried in the earth. The latter results should be comparably valid for a cable with axial current variation induced by the excitation of natural modes. Recently [2] a satisfactory "natural mode" buried cable transmission line model has been developed, so it appears worthwhile to perform a surface cable parameter study within such a transmission line model framework.

Here we shall assume an electric field with 1 volt/meter peak amplitude and a 10 nanosecond rise time incident either longitudinally or vertically with respect to a cable lying along the earth-air interface. The cable is a sheath insulated wire on the order of tens of meters in length. We assume for the transmission line various termination impedances

crudely representative of mobile equipment grounding practices. Cable currents are calculated for several soil conductivities.

2. THE SURFACE CABLE TRANSMISSION LINE MODEL

A cross section of the idealized surface cable model is shown in Figure 1.

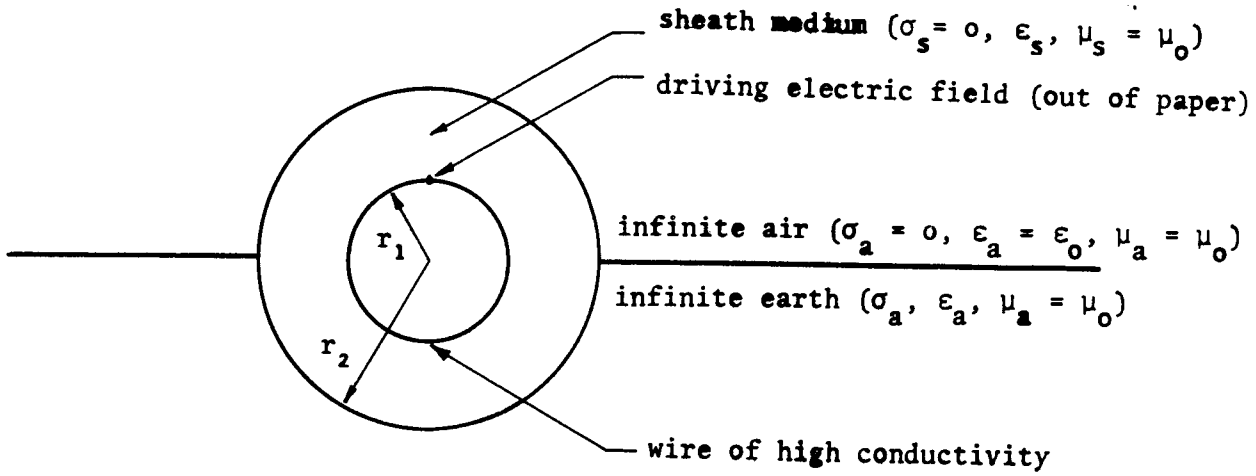

Figure 1. Cross Section of Surface Cable

A transmission line analog to the cable of Figure 1 is shown schematically in Figure 2.

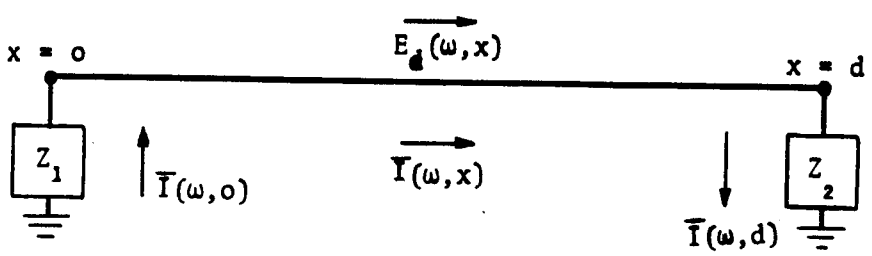

Figure 2. Surface Cable Transmission Line

The driving electric field E_d and the termination impedances Z_1, Z_2 will be discussed shortly. Implied in all of the following is the assumption that the actual incident field suffers negligible attenuation through the insulating sheath and the diameter of the entire cable is much less than a wavelength in the earth medium.

For purposes of Fourier analysis we adopt a harmonic time dependence of $e^{-i\omega t}$. Suppressing line parameter ω dependence, the frequency domain transmission line current equation is:

$$\frac{\partial^2 \overline{I}(\omega,x)}{\partial x^2} + h^2\, \overline{I}(\omega,x) = -YE_d(\omega,x) \quad . \tag{1}$$

The uniformly distributed longitudinal impedance Z and transverse admittance Y determine the propagation constant h and characteristic impedance Z_c:

$$ZY = -h^2 \ , \ Z_c = \sqrt{Z/Y} \quad . \tag{2}$$

In terms of a driving field sufficiently general for the present calculations, the solution of (1) subject to the termination conditions of Figure 2 is:

$$\overline{I}(\omega,x) = F(x) + e^{ihx}\,\frac{[AF(d)e^{ihd} - B\,F(o)]}{[C - De^{2ihd}]} + e^{ih(d-x)}\,\frac{[Ae^{ihd}F(o) - B'F(d)]}{[C - De^{2ihd}]} \tag{3}$$

where,

$$E_d(\omega,x) = E_o(\omega)e^{i\gamma x}, \quad \mathrm{Im}(\gamma) > 0 \quad ;$$

$$F(x) = \frac{E_o}{2Z_c}\left[\frac{(e^{i\gamma x} - e^{ihx})}{i(\gamma - h)} + \frac{(e^{i\gamma d}\, e^{ih(d-x)} - e^{i\gamma x})}{i\,(\gamma + h)}\right] ;$$

and,

$$A = (Z_1 - Z_c)(Z_2 - Z_c)$$

$$B = (Z_2 + Z_c)(Z_1 - Z_c) \ , \quad B' = (Z_1 + Z_c)(Z_2 - Z_c)$$

$$C = (Z_1 + Z_c)(Z_2 + Z_c)$$

$$D = (Z_1 - Z_c)(Z_2 - Z_c) \ .$$

Above, $E_o(\omega)$ denotes the product of the incident field amplitude and some appropriate interface transfer function. A possible $e^{i\gamma x}$ space dependence is "factored out" of the incident field for generality. The time response of the cable is the Fourier integral:

$$I(t,x) = 1/2\pi \int_{-\infty}^{\infty} \bar{I}(\omega,x)e^{-i\omega t}d\omega \quad . \tag{4}$$

For the calculations of this note, (4) was integrated numerically.

Calculating the surface cable h and Z

Guided by our previous results in [1] we shall simply ignore the air medium in Figure 1 for purposes of obtaining a surface cable longitudinal impedance. Thus, we assume

$$Z \approx Z_e \quad . \tag{5}$$

In (5) Z_e is the longitudinal transmission line impedance of the Figure 1 cable buried at "infinite depth" in the soil medium. An approximation of probably comparable validity for the transverse admittance is the familiar estimate $Y \approx Y_e/2$. Thus, for the surface cable propagation constant we assume from (2) that

$$h \approx h_e/\sqrt{2} \quad . \tag{6}$$

A spatially uniform field (one case we consider here) applied to a finite length cable will most certainly excite the natural modes of the cable. In [1] we considered a uniformly illuminated infinite length cable in which case the natural modes cannot be excited. For the calculation of Z_e, h_e in (5) and (6) we utilize the recent model of Hill and Wilson [2] in which accurate parameters of a natural mode buried cable transmission line have been obtained. Rather than needlessly repeat the description of this model, the original article is included in this work as Appendix B. Of course, the latter model produces transmission line parameters for an infinite line so the present calculations contain the usual assumptions regarding the addition of termination conditions to such a line.

The driving electric field

We assume a hypothetical pulse shape for the incident electric field of the form:

$$E_{inc.}(t) = 1.05(e^{-at} - e^{-bt}) \text{ volts/meter}, \tag{7}$$

where $a = 4\times10^6$ and $b = 476\times10^6$. The resultant driving field for the transmission line is in general,

$$E_d(\omega,x) = 1.05\ T(\omega)\ \frac{(a-b)e^{i\gamma x}}{(\omega+ia)(\omega+ib)} \quad . \tag{8}$$

In (8), the transfer function $T(\omega)$ and the propagation constant γ are obtained by calculations assuming the cable not present. We consider two cases:

1) The source of the incident field is directly overhead and the electric vector of (7) lies along the cable. The field (8) is, in this case, assumed to be uniform and hence $\gamma = 0$. From any text discussing the Fresnel coefficients [3] one finds

$$T(\omega)_{overhead} = \frac{2k_a}{k_e + k_a} , \tag{9}$$

where the propagation constants for earth (e) and air (a) are, in our convention,

$$k = \sqrt{\mu\varepsilon\omega^2 + i\mu\sigma\omega} , \quad \mathrm{Im}(k) > 0 .$$

2) The incident field source lies "end-on" with respect to the cable origin and the electric vector of (7) is perpendicular to the ground plane. The surface wave treatment of Stratton [3] is applicable (Appendix A) in this case and we find under reasonable assumptions that

$$T(\omega)_{end\text{-}on} = \frac{k_a}{k_e} ,$$

$$\gamma_{end\text{-}on} = \frac{ik_e k_a}{\sqrt{k_e^2 + k_a^2}} , \quad \mathrm{Im}(\gamma_{end\text{-}on}) > 0 . \tag{10}$$

<u>Termination impedances</u>

For the transmission line termination impedances of Figure 2 we shall adopt a number of possibilities, hopefully encompassing a range of crude correspondence to actual grounding situations of surface cables in mobile defense systems. Some relatively simple terminations should suffice for the present study.

Always of interest are the limiting terminations $Z_1 = Z_2 = 0$ (short circuit) and $Z_1 = Z_2 = Z_c$ (matched loads). A principally resistive impedance results from a vertical ground stake. Sunde [4] gives the following approximation:

$$Z_{stake} \approx \frac{1}{2\pi\ell\sigma_e} [\ln(4\ell/a) - 1] \ , \tag{11}$$

where ℓ is the length and a the radius of the grounding rod.

Finally we consider the sphere shown in Figure 3.

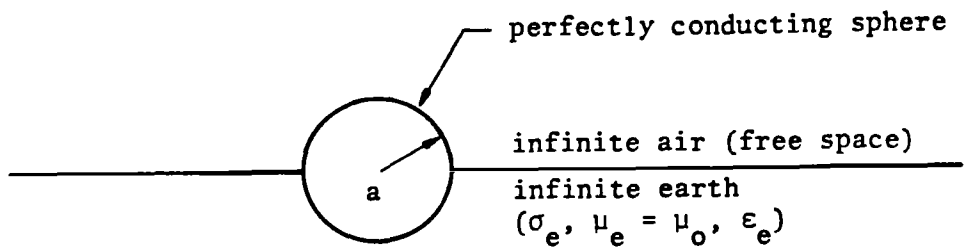

Figure 3. Sphere Termination

The capacitance of the sphere is easily found to be:

$$C = 2\pi a(\varepsilon_o + \varepsilon_e) \ . \tag{12}$$

Including loss due to the soil conductivity, the impedance of the Figure 3 configuration is

$$Z_{sphere} = \frac{i}{2\pi a[(\varepsilon_o + \varepsilon)\omega + i\sigma_e]} \ , \tag{13}$$

A small sphere affords a fairly high termination impedance. A larger sphere may represent equipment vans, et cetera. We should point out, however, that we ignore in this work any pickup to the termination structures.

3. NUMERICAL RESULTS

We consider a typical cable, the specifications of which are (Figure 1):

$r_1 = .9 * .0254$ m

$r_2 = (.9 + .065) * .0254$ m

$\sigma_1 = 5.88 \times 10^7$ mhos/m (copper)

$\varepsilon_s = 2.75\ \varepsilon_o$ (plastic sheath) ; $(\sigma_s = 0)$

All permeabilities are that of free space, and

$\mu_o = 4\pi \times 10^{-7}$ h/m

$\varepsilon_o = 1/36\pi \times 10^{-9}$ f/m

The earth dielectric constant is fixed at

$\varepsilon_e = 10\ \varepsilon_o$.

The remaining parameters (type of incident field, cable length d, observation point x, soil conductivity and assumed terminations) are specified on the plots.

Specific termination impedances considered are:

1) Z_c (characteristic impedance)
2) short
3) sphere (equation 13) with 8 inch radius
4) sphere with 2m radius
5) ground stake (equation 11) 2m long, 1cm radius

Results are displayed in Figures 4-14.

The shorted line (equivalent here to the midpoint of an infinite line) provides the worst case estimates for a given earth conductivity as shown in Figure 4.

Qualitatively, it is useful to consider the approximate transfer functions:

$$T(\omega)_{\text{overhead}} \sim \frac{1-i}{c}\sqrt{\frac{2\omega}{\mu\sigma_e}} \quad , \sqrt{\frac{\varepsilon_e \omega}{\sigma_e}} << 1$$

$$T(\omega)_{\text{end-on}} \sim 1/2\ T(\omega)_{\text{overhead}} \quad . \tag{14}$$

The transfer functions admit $\lesssim$10% of the incident field at 10^6 Hz The line current $\overline{I}(\omega)$ has typically a broad maximum in the range 10^4-10^6 Hz hence the late time tail of the infinite line current. In many cases the σ_e dependence of $T(\omega)$ dominates overall and currents are reduced with increasing soil conductivity. The other higher conductivity examples show also an altered pulse shape due to the σ_e dependence of the termination impedances.

Since the end-on transfer function is so similar to $T(\omega)_{\text{overhead}}$, only a few end-on cases were included. The end-on current results (allowing for the time delay $\sim x/c$) are roughly just 1/2 the corresponding overhead incidence currents and exhibit similar pulse shapes. The phase velocity associated with h is << c. The attenuation from h, however, dominates that of γ (equation 10). Thus, except for the time delay, the end-on results for short cables are not very sensitive to γ. We have explicitly verified the latter points by calculating the end-on cases with $\gamma = 0$.

4. CONCLUSIONS

Encompassing all of the cases considered, the simple surface cable model predicts cable currents of amplitude ~(3-20) amps/kv with rise time ~(.1-.2)μsec, given the incident double exponential pulse with 10 ns rise time. The surface wave approximation of an end-on EMP

source yields peak currents ~1/2 the amplitude of currents resulting from uniform overhead illumination of the cable. In many cases the cable currents decrease with increasing soil conductivity, due to the $\sigma_e^{-1/2}$ dependence of the earth-air interface transfer functions.

Although the results are reasonable, a number of simplifying assumptions have been made. It would be desirable to experimentally test the model under favorable situations of incident pulse, termination impedances and soil conductivity. The estimates presented here should also provide a useful comparison to predictions of more sophisticated models which could be developed for the surface cable problem.

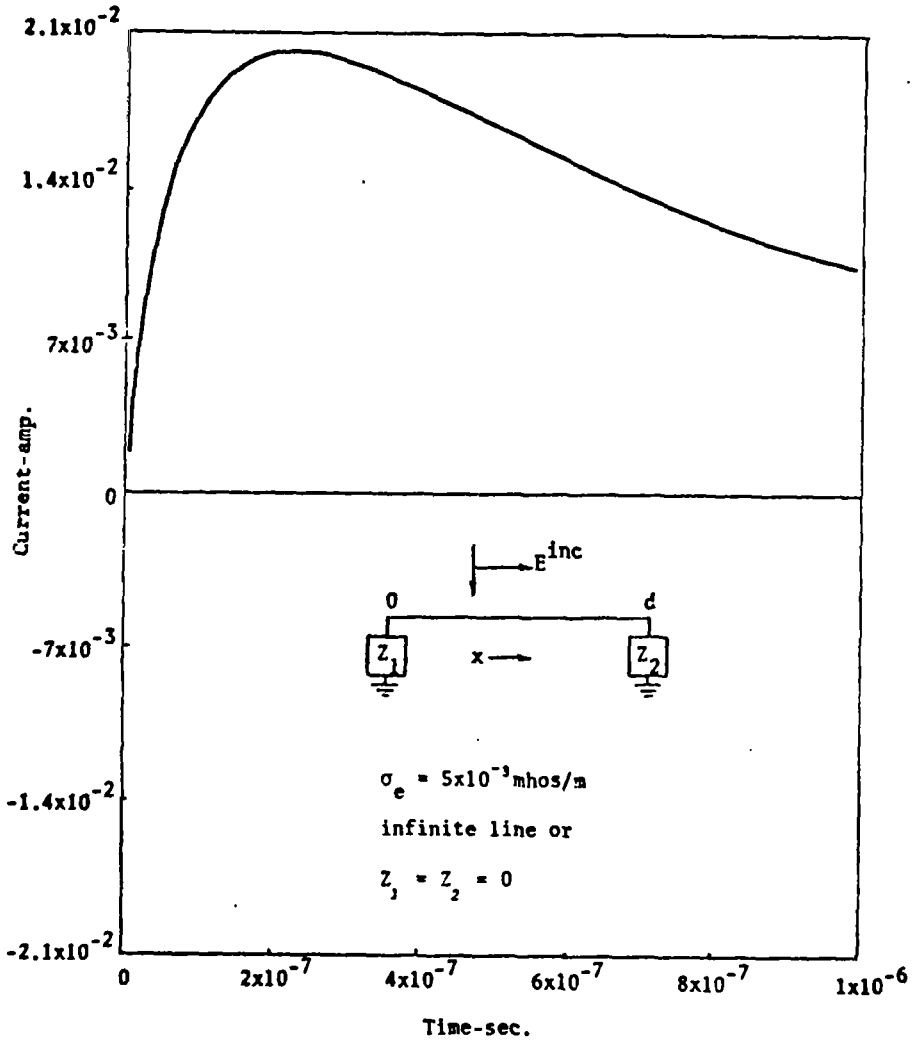

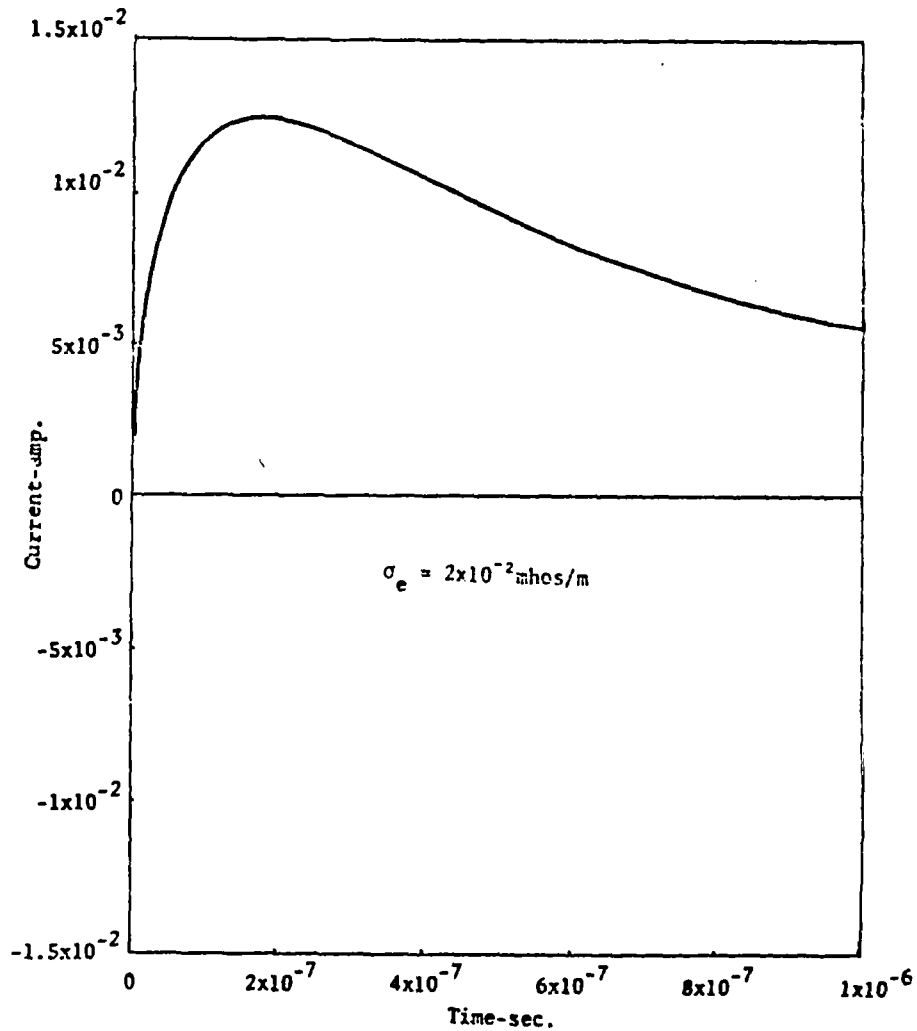

Figure 4. Cable Current vs. Time.

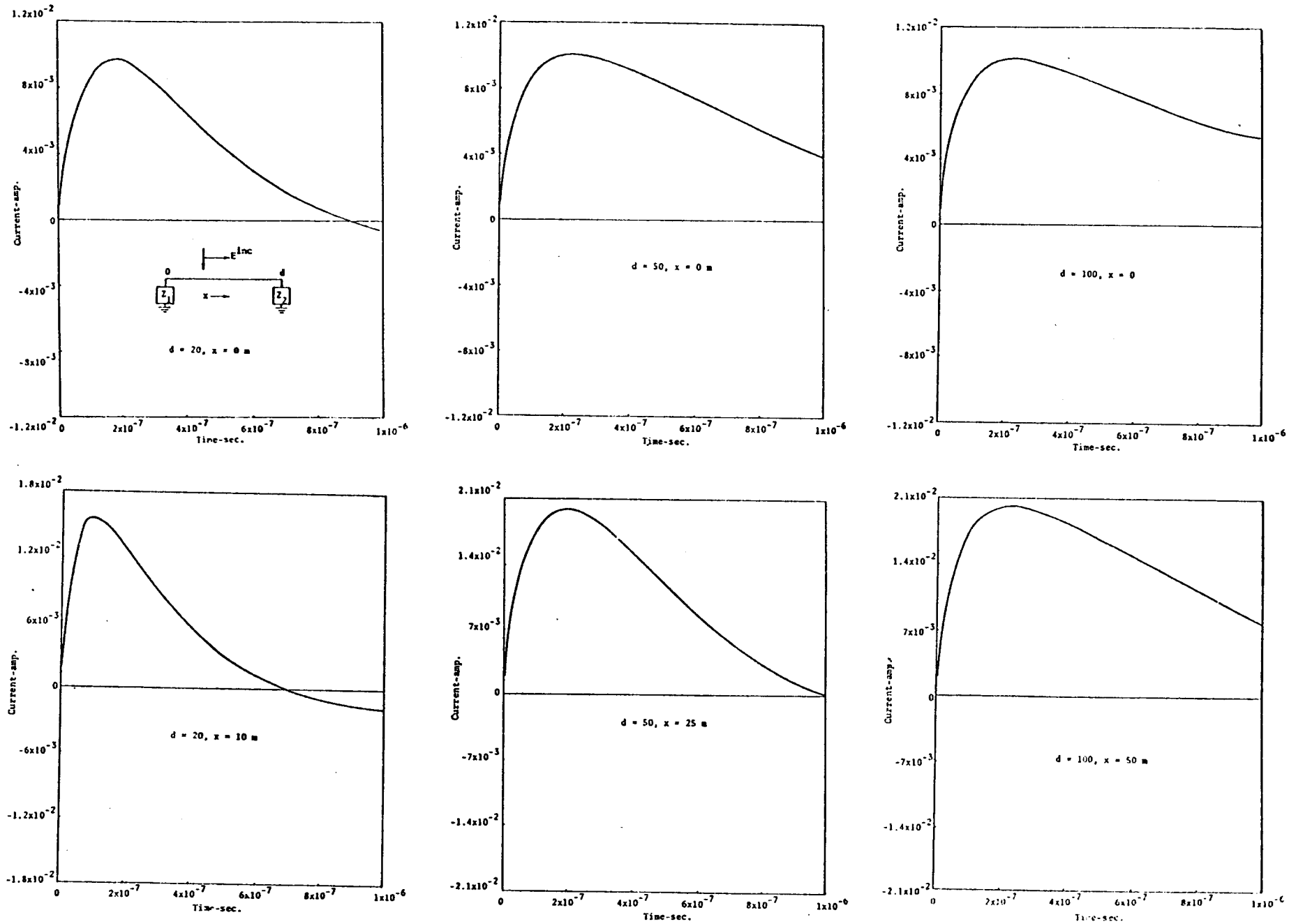

Figure 5. Cable Current vs. Time. $Z_1 = Z_2 = Z_c$, $\sigma_e = 5\times10^{-3}$ mhos/m.

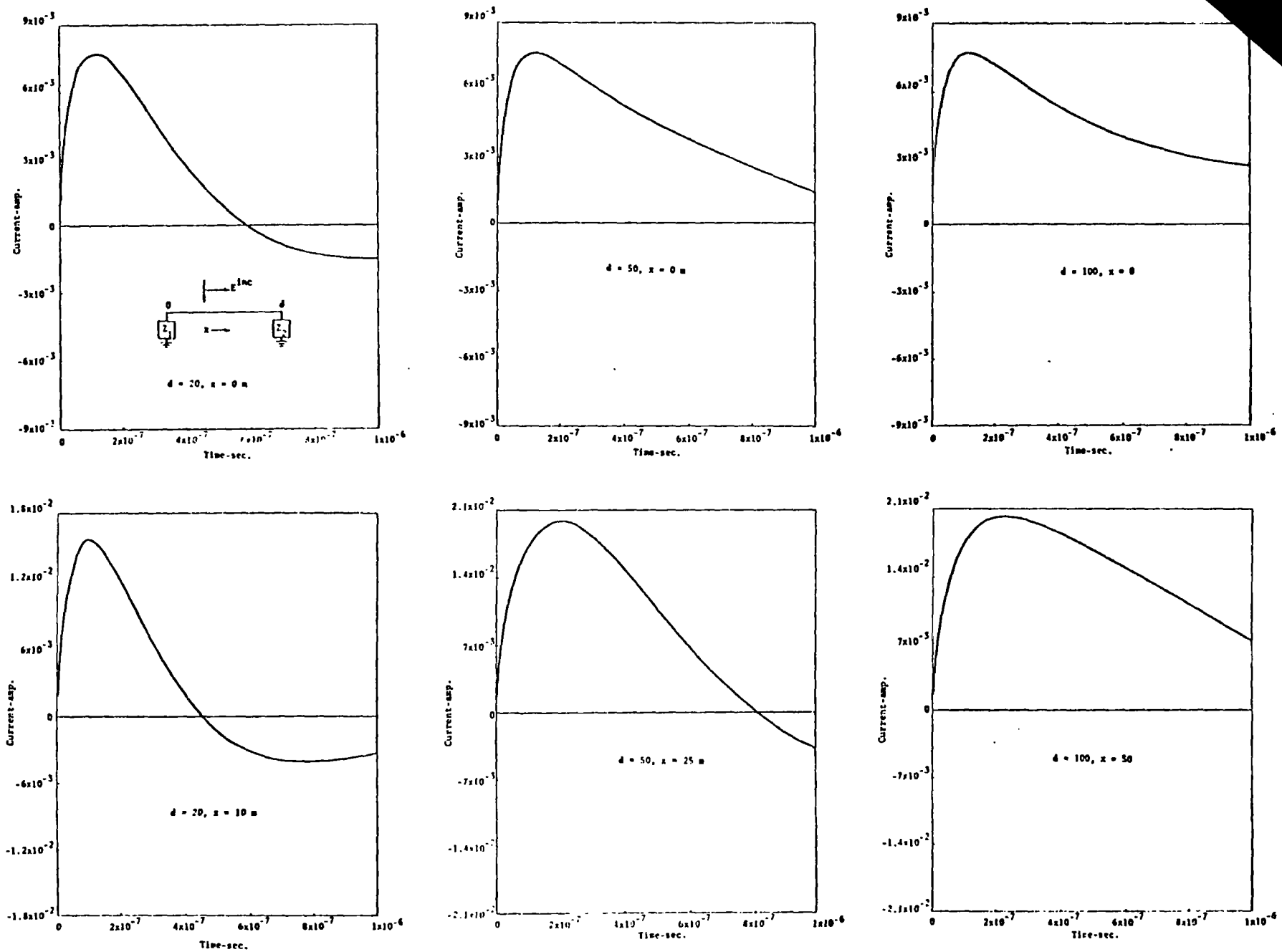

Figure 6. Cable Current vs. Time. $Z_1 = Z_2 = 2$ m ground stake, $\sigma_e = 5\times10^{-3}$ mhos/m,

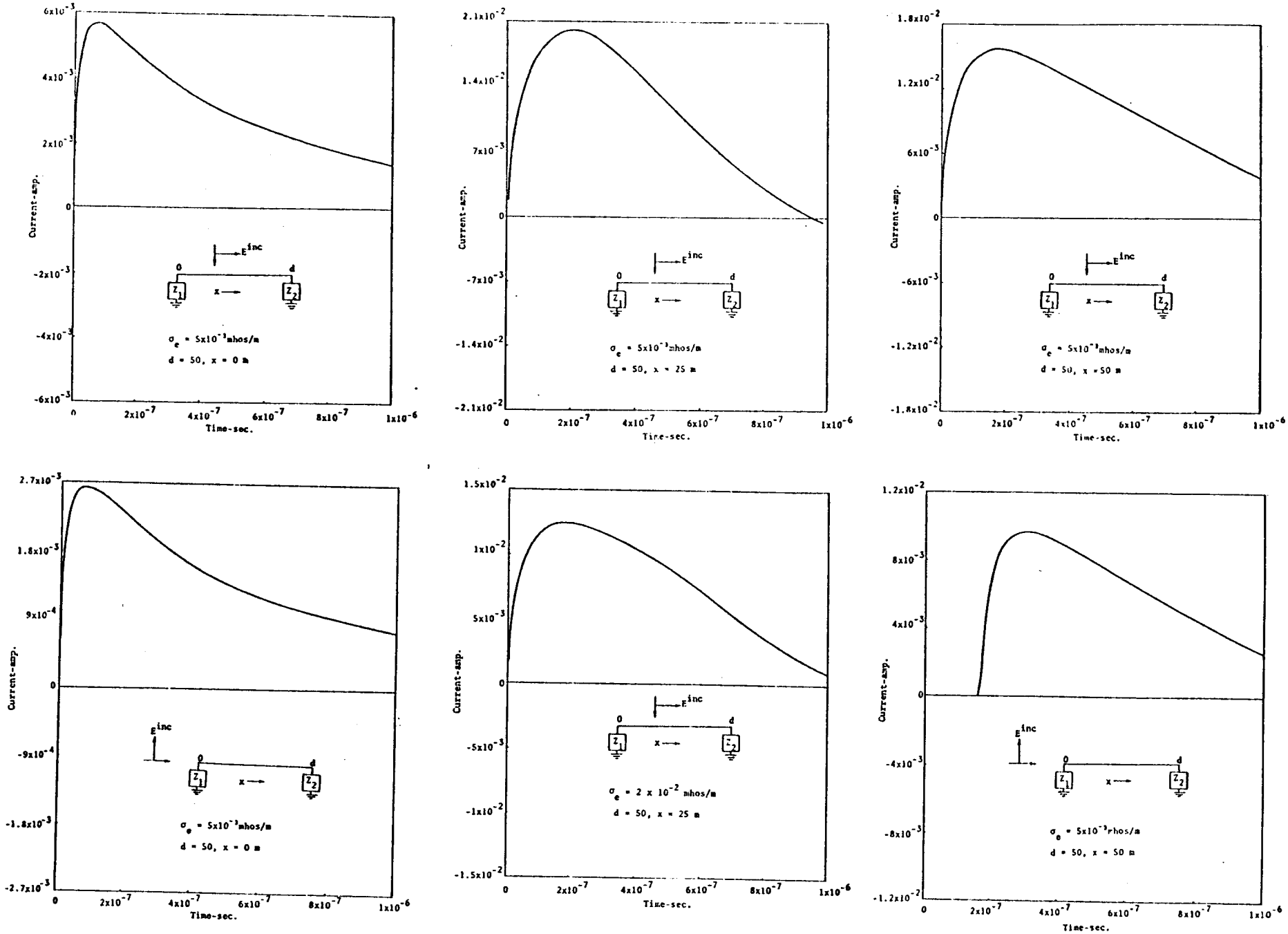

Figure 7. Cable Current vs. Time. Z_1= sphere with 8-inch radius, Z_2= sphere with 2 m radius,

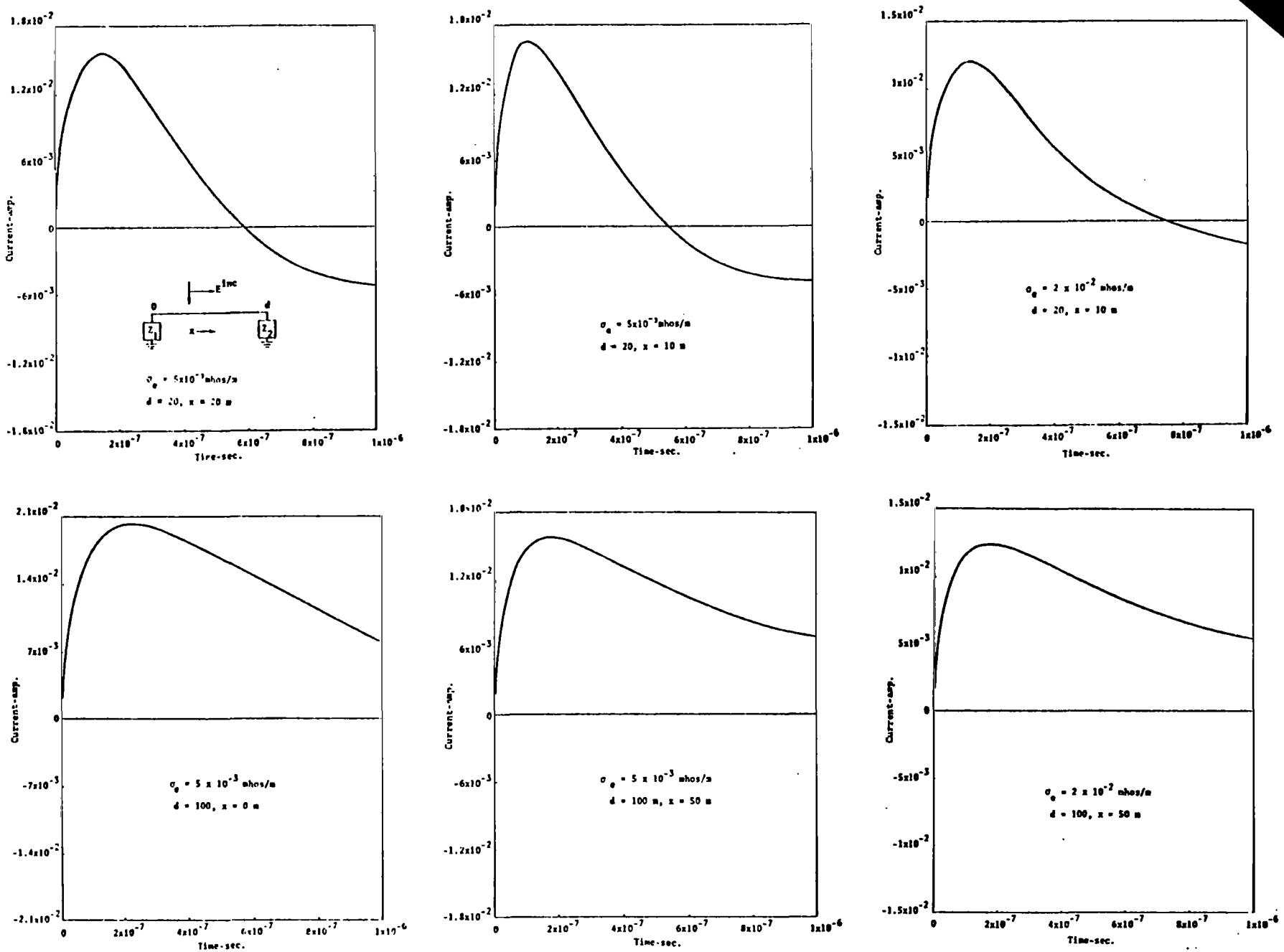

Figure 8. Cable Current vs. Time. Z_1= sphere with 8-inch radius, Z_2= sphere with 2-m radius.

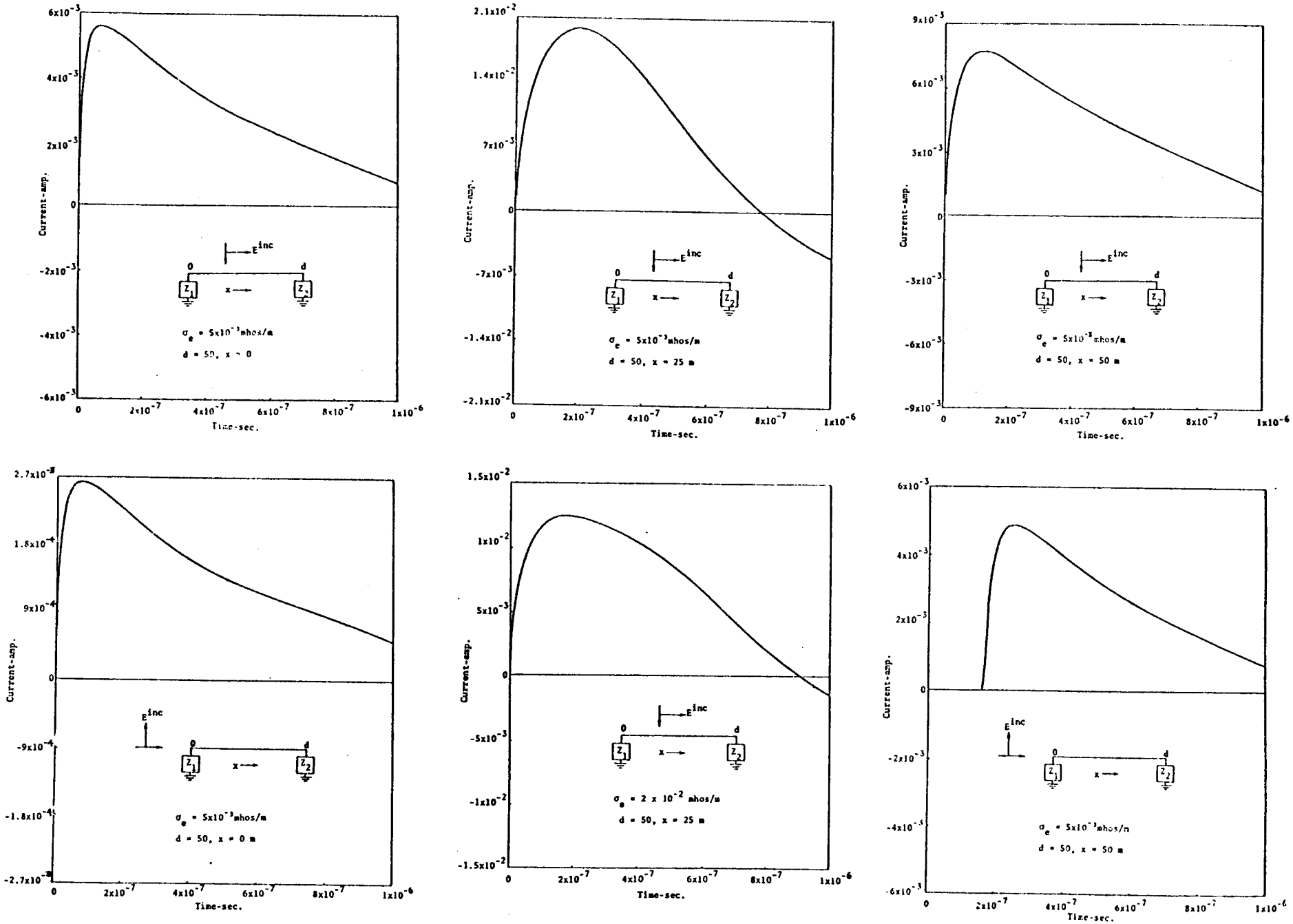

Figure 9. Cable Current vs. Time. Z_1= sphere with 8-inch radius, Z_2= 2-m ground stake.

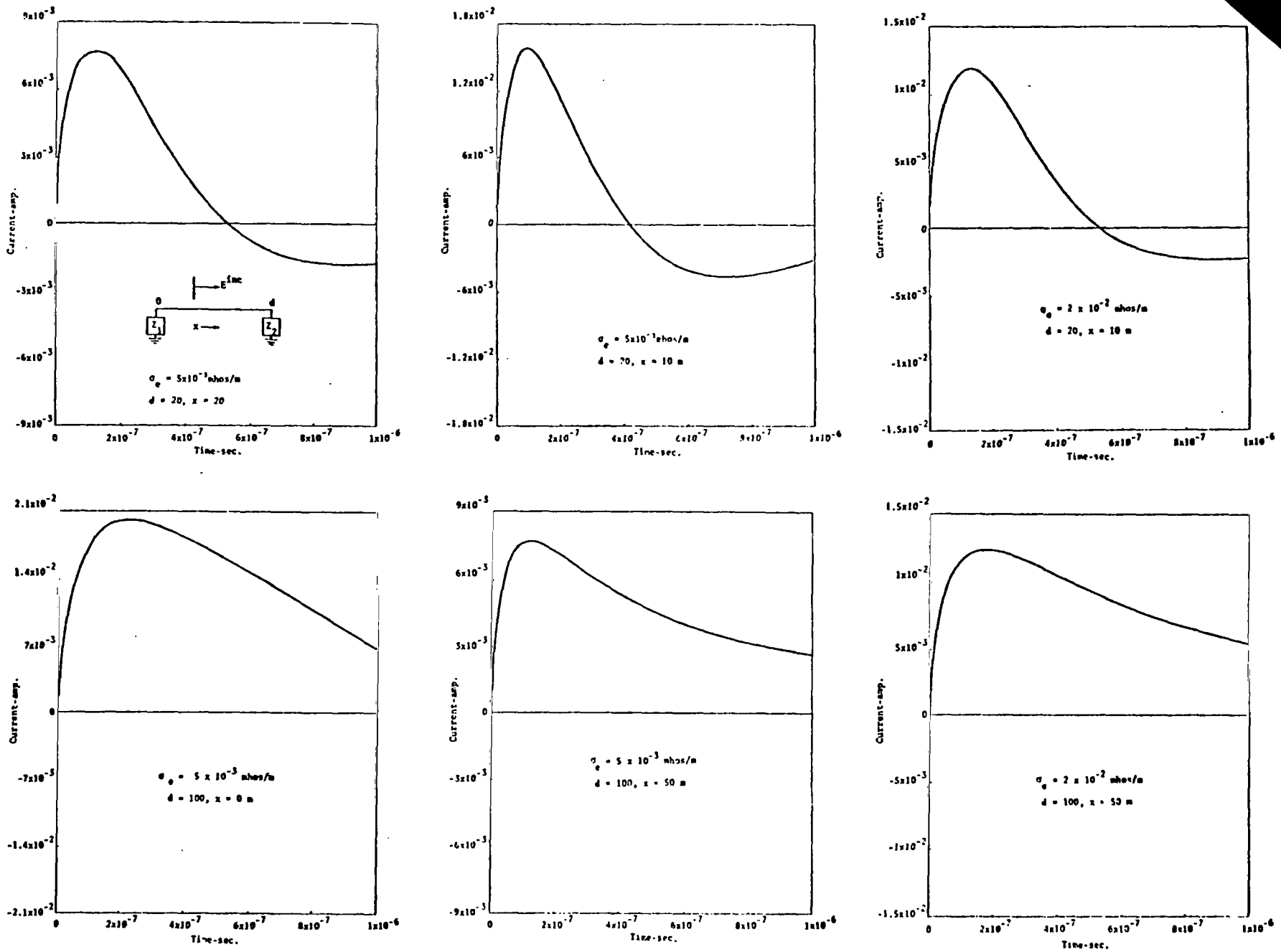

Figure 10. Cable Current vs. Time. Z_1= sphere with 8-inch radius. Z_2= 2-m ground stake.

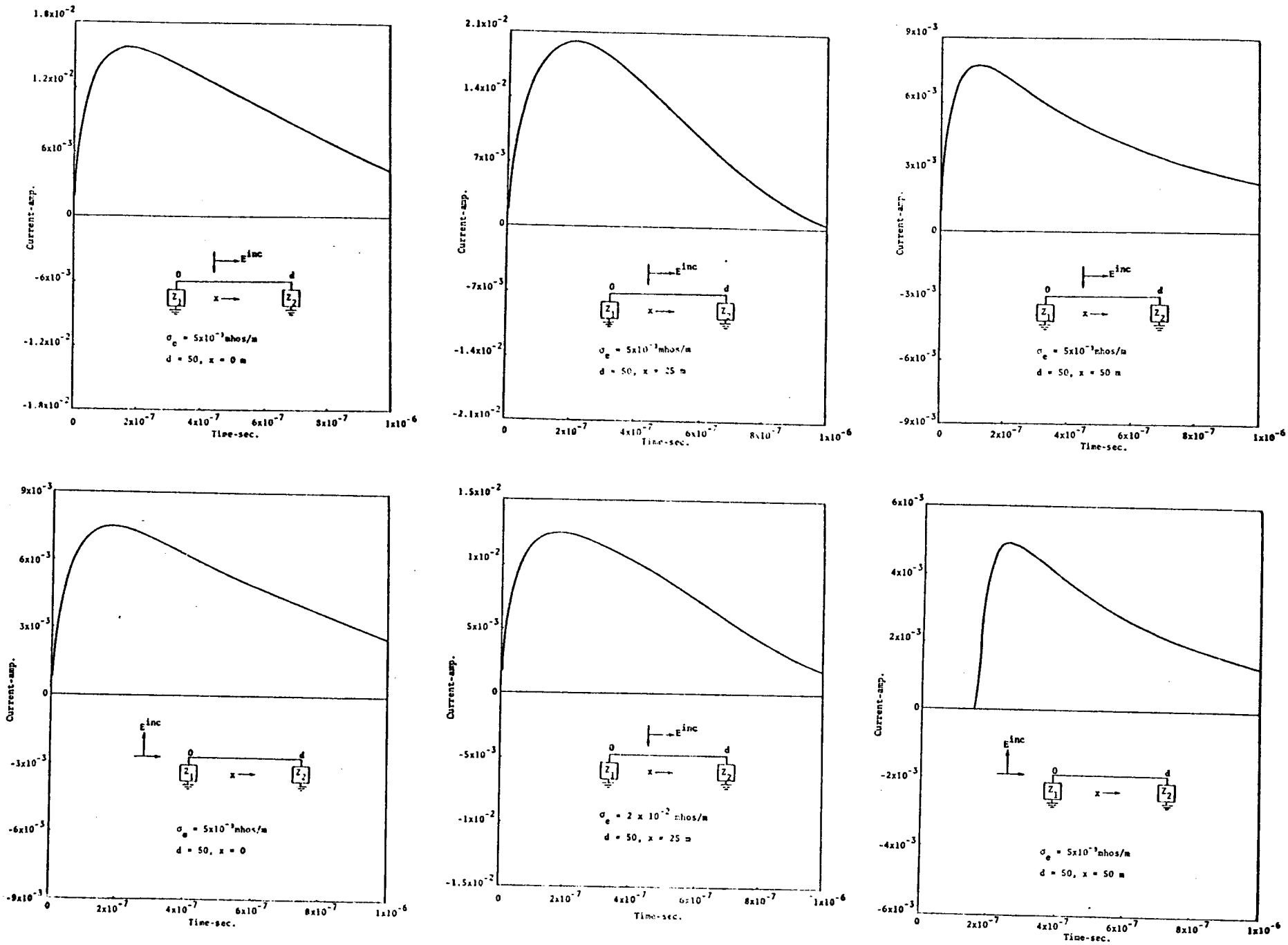

Figure 11. Cable Current vs. Time. Z_1= sphere with 2-m radius, Z_2= 2-m ground stake,

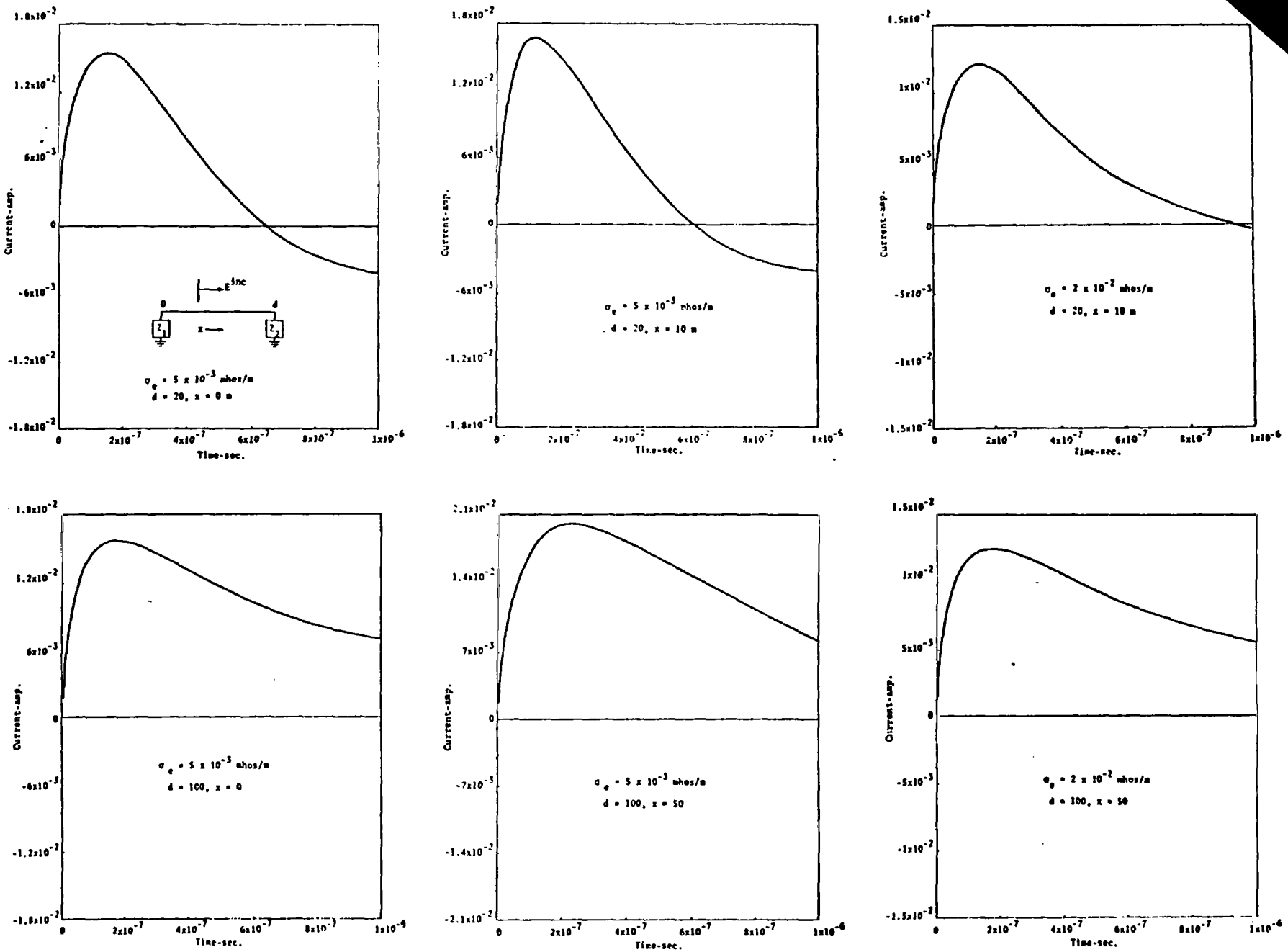

Figure 12. Cable Current vs. Time. Z_1= sphere with 2-m radius, Z_2= 2-m ground stake,

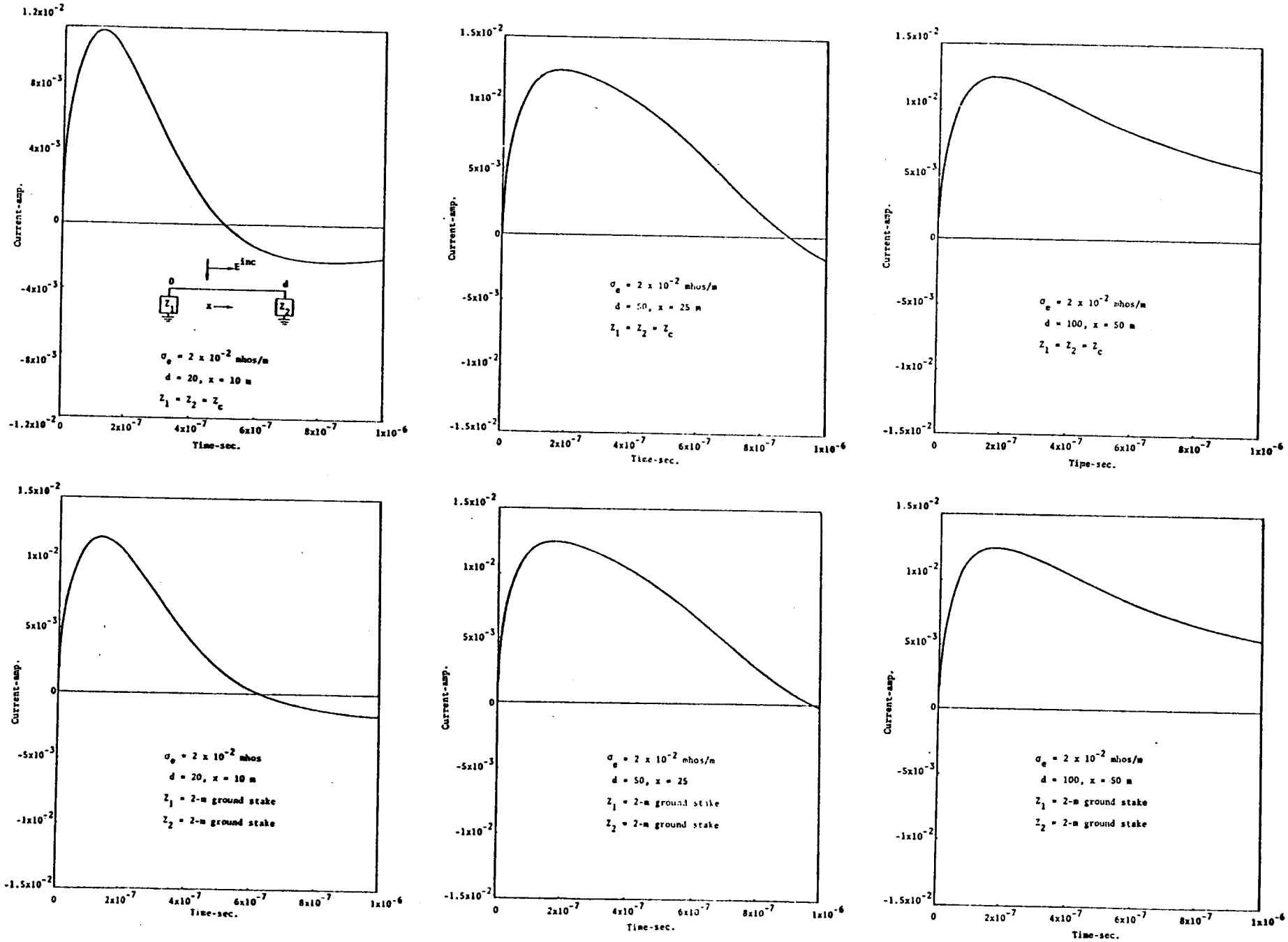

Figure 13. Cable Current vs. Time.

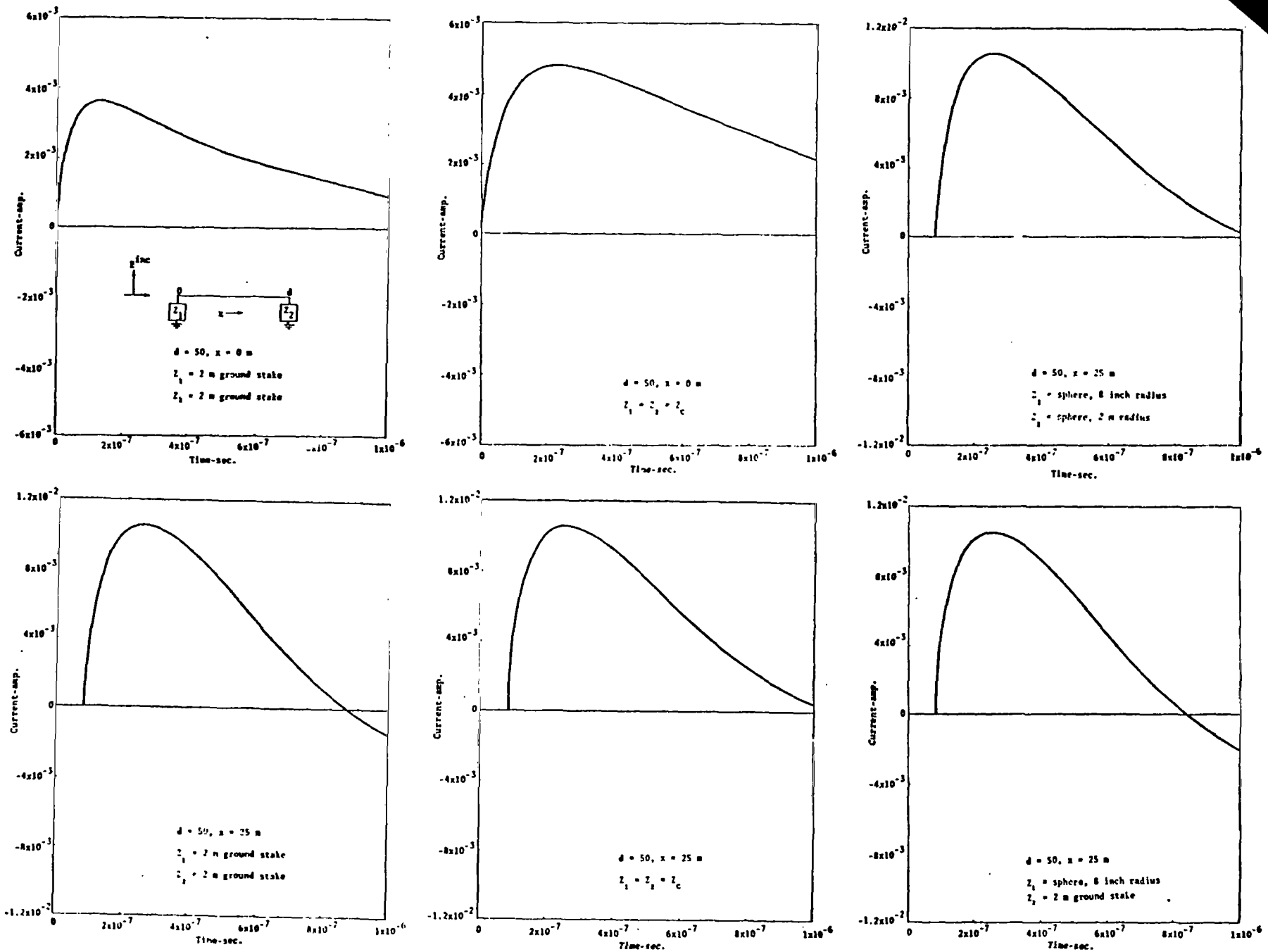

Figure 14. Cable Current vs. Time. $\sigma_e = 5\times10^{-3}$ mhos/m.

APPENDIX A

TRANSFER FUNCTION FOR END-ON ILLUMINATION

Stratton [3, page 516] presents a detailed discussion of TM surface waves traveling along the earth-air interface. We shall simply adapt his notation and results for our purposes. The situation is that of inhomogeneous plane waves and a complex angle of incidence θ_0 such that no reflected wave occurs. The refracted electric field component along the interface is our desired drive field for the transmission line.

The surface wave geometry is shown in Figure A-1.

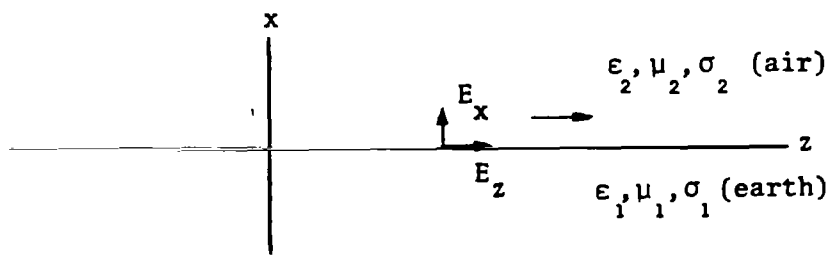

Figure A-1. Surface Wave Geometry

At the interface as $x \to 0+$, the field solutions are

$$E_x = \frac{\omega\mu_2}{k_2} \sin\theta_0 C \; e^{ik_2 \sin\theta_0 z - i\omega t} \tag{1}$$

$$E_z = \frac{\omega\mu_2}{k_2} \cos\theta_0 C \; e^{ik_2 \sin\theta_0 z - i\omega t} \tag{2}$$

where C is an arbitrary constant and

$$\cot \theta_0 = \frac{k_2}{k_1} \quad (\text{for } \mu_2 = \mu_1) \quad . \tag{3}$$

We equate at $z = 0$ the vertical field E_x of (1) and our incident field $\overline{E}_{inc}(\omega)e^{-i\omega t}$ thereby fixing C. The "driving field" E_z from (2) is thus:

$$E_z = \left(\frac{k_2}{k_1}\right) \overline{E}_{inc}(\omega)e^{i\gamma z} \quad , \tag{4}$$

where

$$\gamma = \frac{ik_1 k_2}{\sqrt{k_1^2 + k_2^2}} \quad , \ \mathrm{Im}(\gamma) > 0 \quad . \tag{5}$$

The restriction on γ in (5) insures exponential decay, given our $e^{-i\omega t}$ convention.

The assumption made above is that some source far from the cable origin ($z = 0$ here) has established (in a manner we need not specify) a TM surface wave. By limiting the problem to the interface ($x = 0$) we may approximately fix the surface wave amplitude consistent with ignoring the presence of the cable. As demonstrated in Stratton, the planes of constant phase are perpendicular to the interface in the limit of a perfectly conducting earth. The phase planes of an actual surface wave are tilted forward, though for the earth conductivities we consider, the tilt angle is small for frequencies $\lesssim 10^6$ Hz.

APPENDIX B

NATURAL MODE BURIED CABLE MODEL

The following article [2] is an essentially preliminary study though it presents a satisfactorily complete formulation of the transmission line model for calculational purposes. The conclusions regarding the "transverse conductance anomaly" are far too restrictive, however. In a forthcoming paper, the authors of [2] shall demonstrate that the model actually yields a close approximation to the results of a "forced oscillation" analysis (independent of transmission line ideas) even though the original equivalent circuit for the transmission line cannot always be physically realized at sufficiently high frequencies.

DRAFT

BURIED CABLE TRANSMISSION LINE PARAMETERS:

A COMPARISON OF TWO THEORETICAL MODELS

J. R. Hill

M. R. Wilson

March 1973

APPENDIX B

AMRC-N-9

TRANSIENT CURRENT ESTIMATES
FOR FINITE LENGTH SURFACE CABLES

Originally
Prepared For

Mc Donnell Douglas Corporation

Under Contract

DAHC60-72-C-0080

DRAFT

TABLE OF CONTENTS

Section		Page
1	Introduction	B-1
2	Transmission Line Equations	B-3
3	Natural Mode Analysis	B-7
4	Marston-Graham Model	B-12
5	Numerical Comparison	B-23
6	Conclusions	B-39
Appendix	Transmission Line Circuit For the Bare Wire	B-40
References		B-46

SECTION 1

INTRODUCTION

In 1966 Marston and Graham (reference 1) presented an approximate procedure for the estimation of transmission line parameters appropriate to a buried conducting cable with an insulating sheath. We have solved the more exact model which the Marston-Graham (MG) method approximates and shall demonstrate a striking disagreement between the results of the two treatments. Noting the presence of an interpretative difficulty in the original MG model, we shall further show that a plausible modification of one of the MG assumptions results in quite reasonable qualitative agreement with all of the line parameters calculated from the more elaborate treatment.

We consider in this note an insulated cylindrical conductor surrounded by an infinite, lossy dielectric medium. For this situation, one may define transmission line parameters via the fields of a natural mode (free oscillation) analysis. Such a "more exact" approach to the buried cable is not a new idea, but to our knowledge, complete numerical predictions of the natural mode buried cable model have not been previously published. Several authors have discussed (references 2 and 3) the longitudinal propagation constant but [they] did not explicitly calculate transmission line impedances from the "exact" fields. In order to obtain a perhaps more realistic transmission line model and, as a basis for comparison with more approximate methods, we calculate all line quantities from the numerical solution of the boundary value problem.

The three-media natural mode problem involves the numerical solution of a rather complicated transcendental equation. One may

avoid the solution of this equation by constructing an approximate sheathed wire model from the fields of a bare wire embedded in an infinite dielectric. Such a procedure was utilized by MG and the modified version of [their] model, with relative computational simplicity, should provide more reliable engineering estimates.

If the conductivity of the infinite "earth" medium is sufficiently low, the calculated transmission line transverse conductance exhibits anomalous behavior at high frequencies. Such behavior appears to indicate theoretical limitations of the model. Fortunately, for practical current calculations on long cables, the anomaly occurs at frequencies high enough so as not to contribute significantly to the bulk current.

The next section is a review of the transmission line circuit and equations appropriate to our physical model. Section 3 outlines the free oscillation analysis and the calculation of transmission line parameters from the field solutions. In section 4, we critically review the MG construction of a sheathed wire model approximating that of section 3. Numerical results are presented and discussed in section 5. Conclusions follow in section 6.

2. TRANSMISSION LINE EQUATIONS

The theory of transmission lines is treated in references (4,5,6). An incremental section of the general model we wish to consider is shown in Figure 1.

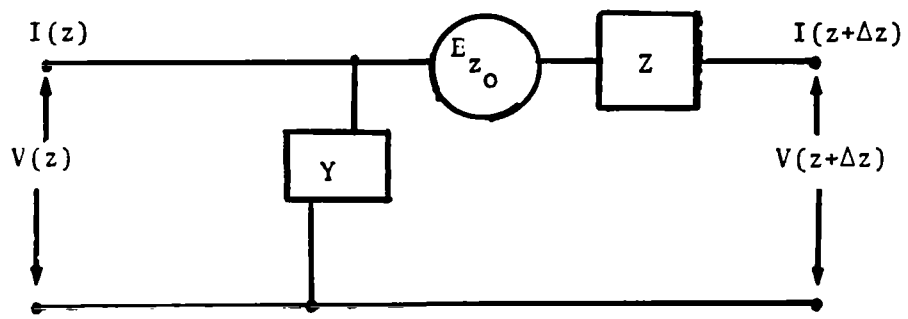

Figure 1. Incremental Section of Transmission Line

The impedance parameters of Figure 1 are assumed to be uniformly distributed along the line. The longitudinal impedance is Z and Y is the transverse admittance. A driving electric field E_{z_o} may be present.

Choosing the propagation convention $e^{-i\omega t}$ we have in the frequency domain:

$$Z = R - i\omega L \tag{1}$$

$$Y = G - i\omega C \ . \tag{2}$$

R, L, G and C are respectively the series resistance, series inductance, shunt conductance and shunt capacitance, all per unit length and frequency dependent. Subsequent equations will not explicit the ω dependence.

Application of Kirchoff's voltage and current rules to the incremental transmission line section yields the basic two equations,

$$\frac{\partial V}{\partial z} = -ZI + E_{z_o} \tag{3}$$

$$\frac{\partial I}{\partial z} = -VY \quad . \tag{4}$$

Combining (3) and (4) one obtains the current equation:

$$\frac{\partial^2 I}{\partial z^2} - ZYI = -E_{z_o} Y \quad . \tag{5}$$

Introducing the characteristic impedance Z_c and the propagation constant h the following four transmission line parameters may be calculated given any two of them:

$$h^2 = -YZ \tag{6}$$

$$Z_c^2 = Z/Y \tag{7}$$

$$Z = -ihZ_c \tag{8}$$

$$Y = -ih/Z_c \quad . \tag{9}$$

By combinations of the homogeneous solutions $\left(\propto e^{\pm ihz} \right)$ of equation (5) appropriate to desired boundary conditions, complete solutions to (5) are easily obtained. The source term, $-E_{z_o} Y$, enters through a particular integral.

In this paper, we examine the calculation of the four quantities in equations (6-9). The corresponding physical model consists of a cylindrical conductor covered with an insulating coaxial sheath and surrounded by an infinite, lossy dielectric medium.

The specific transmission line analog to our physical model is shown below in Figure 2.

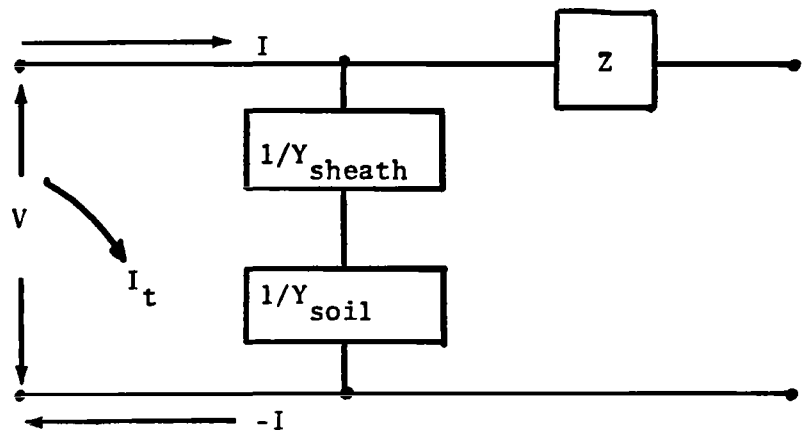

Figure 2. Coaxial Transmission Line Section

A transverse current (per unit axial length) I_t returns through the sheath and the infinite soil, each region given a transverse impedance and corresponding transverse admittance. The total transverse admittance as in Figure 1 is just

$$Y = \frac{Y_{sheath}\, Y_{soil}}{Y_{sheath} + Y_{soil}} \tag{10}$$

From (4) it is evident that:

$$I_t = -\frac{\partial I}{\partial z} \quad . \tag{11}$$

Note that we have indicated no driving field in the circuit model of Figure 2. In the usual approach to this problem one relates the transmission line parameters to solutions of Maxwell's equations obtained in the absence of a driving field. The resulting Z and Y are then assumed to give an adequate description of the driven line through

the solution of (5). This assumption is reasonable due to the fact that in most cases of interest, a single mode will predominate in the current excited on the line by an incident field.

3. NATURAL MODE ANALYSIS

The geometry of the physical model is shown in Figure 3.

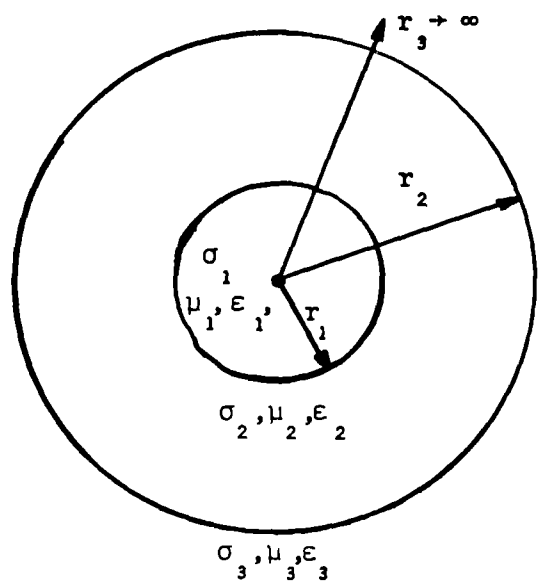

Figure 3. Cable Geometry

The central cable of radius r_1 is assembled to be typically a very good conductor. Region 3, a homogeneous, lossy dielectric, crudely simulates an infinite "earth" medium and constitutes the return circuit of a coaxial system. The insulating sheath, region 2, is allowed a conductivity σ_2. For all media, the unrestricted propagation constants are:

$$k_j^2 = \varepsilon_j \mu_j \omega^2 + i\sigma_j \mu_j \omega; \; j = 1, 2, 3 \quad . \tag{12}$$

If I is the total current in the central conductor and I_o its amplitude we may assume:

$$I = I_o e^{ihz - i\omega t} \quad . \tag{13}$$

The axial propagation constant h of (13) is to be determined by solving the natural mode boundary value problem. Among the many treatments in the literature, Stratton (reference 7) is particularly detailed on cylindrical problems of this nature. For completeness, however, we shall sketch the derivation in the following.

We assume that only symmetric, transverse magnetic modes need be considered. Asymmetric modes would suffer extreme attenuation for the frequencies and lengths $r_2 - r_1$ of interest to us.

The symmetric cylindrical wavefunction (axial component of the Hertz vector) is:

$$\psi_{hk} = Z_o(\lambda r)\, e^{ihz - i\omega t}$$

$$\lambda^2 = k^2 - h^2 \tag{14}$$

Above, $Z_o(\lambda r)$ is a linear combination of zero order Bessel (J_o) or Neumann (Y_o) functions appropriate to each of the three regions of Figure 3. Our notation and definitions of cylinder functions is that of reference (8).

The tangential H, radial E and axial E fields are respectively given by:

$$H_\theta = \frac{ik^2}{\mu\omega} \frac{\partial \psi_{hk}}{\partial r}$$

$$E_r = Z_z H_\theta, \quad E_z = -Z_r H_\theta \quad . \tag{15}$$

Following Stratton's notation, the wave impedances in (15) are:

$$Z_r = \frac{-\omega\mu\lambda}{ik^2} \frac{Z_o(\lambda r)}{\frac{\partial Z_o(\lambda r)}{\partial(\lambda r)}} \quad , \quad Z_z = \frac{\omega\mu h}{k^2} \quad . \tag{16}$$

In region 1, a finite $\psi_{hk}^{(i)}$ may be proportional to $J_o(\lambda_1 r)$ only. Integrating $\sigma_1 E_z^{(i)}$ over the cross section of the central conductor one easily obtains:

$$H_\theta^{(i)} = \frac{-ik_1^2 I}{2\pi r_1 \omega\mu_1 \sigma_1} \frac{J_1(\lambda_1 r)}{J_1(\lambda_1 r_1)} \quad . \tag{17}$$

For regions 2 and 3 we may write:

$$H_\theta^{(2)} = \frac{-ik_2^2}{\omega\mu_2\lambda_2} \left[AJ_1(\lambda_2 r) + BY_1(\lambda_2 r)\right] e^{ihz-i\omega t} \tag{18}$$

$$H_\theta^{(3)} = \frac{-ik_3^2}{\omega\mu_3\lambda_3} CH_1^{(i)}(\lambda_3 r) e^{ihz-i\omega t} \quad . \tag{19}$$

By our convention Im(h) must be positive. In region 3, we choose $\mathrm{Im}(\lambda_3) > 0$ and thus the Hankel function of the first kind in (19) insures vanishing fields at infinity.

The ratio A/B and hence the coefficient C follows from the homogeneous boundary conditions requiring continuous axial E, tangential H at both $r=r_1$ and $r=r_2$. The result is:

$$-A/B = \frac{Y_o(\lambda_2 r_1) - \Gamma Y_1(\lambda_2 r_1)}{J_o(\lambda_2 r_1) - \Gamma J_1(\lambda_2 r_1)}$$

$$= \frac{Y_o(\lambda_2 r_2) - \dfrac{\mu_3\lambda_3 k_2^2}{\mu_2\lambda_2 k_3^2} \dfrac{H_o^{(1)}(\lambda_3 r_2)}{H_1^{(1)}(\lambda_3 r_2)} Y_1(\lambda_2 r_2)}{J_o(\lambda_2 r_2) - \dfrac{\mu_3\lambda_3 k_2^2}{\mu_2\lambda_2 k_3^2} \dfrac{H_o^{(1)}(\lambda_3 r_2)}{H_1^{(1)}(\lambda_3 r_2)} J_1(\lambda_2 r_2)} \tag{20}$$

where,

$$\Gamma = \frac{\mu_1 \lambda_1 k_2^2 J_0(\lambda_1 r_1)}{\mu_2 \lambda_2 k_1^2 J_1(\lambda_1 r_1)} \approx \frac{-(1+i)\, k_2^2}{\mu_2 \lambda_2} \sqrt{\frac{2\mu_1}{\sigma_1 \omega}} \quad . \tag{21}$$

The approximate form of Γ in (21) is suitable for an excellent conductor in region 1 with $\lambda_1 \approx k_1 >> 1$.

The propagation constant h (for given ω) is a root of the transcendental equation (20). Of the infinite roots of (20) one desires that value of h corresponding to minimum attenuation (principal wave).

We employed a regula falsi technique for the numerical determination of h. The root locus $h(\omega)$ was tracked by linear extrapolation from previous roots. Numerical results are discussed in a later section.

Given the roots h of (20), the coefficient ratio A/B and hence the fields are determined through the relations previously noted. It remains to calculate the characteristic impedance Z_c for the transmission line analog to Figure 3 as illustrated in Figure 2.

By definition, the characteristic impedance of our model is

$$Z_c = \left[\int_{r_1}^{r_2} E_r^{(2)}(r)\, dr + \int_{r_2}^{\infty} E_r^{(3)}(r)\, dr \right] I^{-1} \quad . \tag{22}$$

The bracketed factor is the transverse voltage at any point along the line.

Performing the radial integrations in (22) we obtain:

$$Z_c = \frac{-ih\lambda_1 J_o(\lambda_1 r_1)}{2\pi r_1 \sigma_1 \lambda_2^2 J_1(\lambda_1 r_1)} \tag{23}$$

$$\frac{-ihk_1^2\mu_2}{4\mu_1\sigma_1 k_2^2}\left[\frac{k_2^2-k_3^2}{\lambda_3^2}\right]\left\{\begin{array}{l}\left[J_o(\lambda_2 r_2)Y_o(\lambda_2 r_1)-J_o(\lambda_2 r_1)Y_o(\lambda_2 r_2)\right] \\ -\Gamma\left[J_o(\lambda_2 r_2)Y_1(\lambda_2 r_1)-J_1(\lambda_2 r_1)Y_o(\lambda_2 r_2)\right]\end{array}\right\}.$$

The constant Γ in (23) is that of (21). The first term of Z_c is a "skin" impedance and for $\lambda_1 \sim k_1 >> 1$ it represents only a small correction to the second term. For a good conductor such as copper the effects of finite conductivity ($\Gamma \neq 0$) are quite small both in the second term of (23) and in the determination of h from the determinantal equation (20).

Thus, by taking the normal mode h as our transmission line propagation constant and, having defined the characteristic impedance of (23), we may obtain the Z and Y of the line from (8) and (9) respectively. Equivalently we could obtain the total admittance from (10). Given a current of the form in (13) and using (11), the transverse current I_t is -ihI. The individual admittances of Figure 2 are just

$$Y_{sheath} = \frac{-ihI}{\int_{r_1}^{r_2} E_r^{(2)}(r)\, dr} \quad , \quad Y_{soil} = \frac{-ihI}{\int_{r_2}^{\infty} E_r^{(3)}(r)\, dr} \quad . \tag{24}$$

An approximate form of the decomposition of Y in (24) is employed by Marston and Graham. We proceed to a discussion of their model in the next section.

4. MARSTON-GRAHAM MODEL

The solution of the three-media transcendental equation (20) in Section 3 is, in general, a complicated affair. One would like to approximate the model of the previous section in such a way as to avoid (20) altogether. In reference (1), Marston and Graham (MG) have formulated an approximation to the transmission line model of Figure 2 based on the field structure about a good conductor embedded in an infinite, lossy dielectric medium. One naturally assumes that the bare wire fields are similar enough to the fields of the sheathed wire that one may at least estimate the longitudinal impedance and the admittance through the soil of the coaxial transmission line model.

In the following we shall first review the bare wire boundary value problem then restate the original MG prescription for approximating the coaxial model. A difficulty of interpretation will be noted in the MG assumption regarding the longitudinal impedance. The removal of this difficulty by a simple, physically plausible modification will be shown to result in a marked improvement of agreement between the calculated parameters of Section 3 and the corresponding MG approximate values. The graphical numerical comparisons in Section 5 will clearly illustrate the previous statement.

Fields of the Bare Wire

The geometry and notation for the bare wire problem is shown in Figure 4.

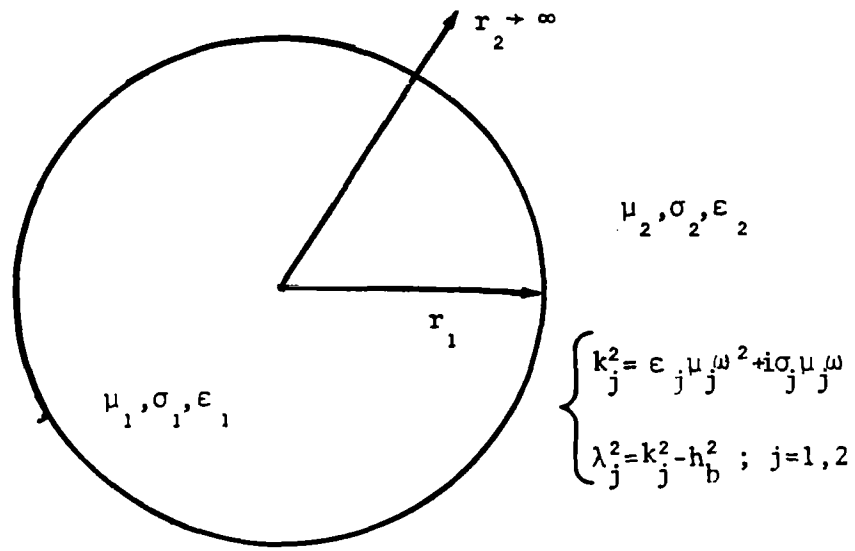

Figure 4. Bare Wire

The classic investigation of the free oscillation modes of the conducting cylinder embedded in dielectric was done by Sommerfeld (reference 9) in 1899. The problem is solved by the method of Section 3 and as before, only axially symmetric TM modes need be considered. To avoid confusion we shall denote the axial propagation constant for the bare wire as h_b. All other definitions and conventions are the same as those of the previous section.

The assumed current in the wire is

$$I = I_o e^{ih_b z - i\omega t} \quad . \tag{25}$$

The TM field solutions for the outer region 2 ("earth" medium) are

$$E_z^{(2)} = \frac{\mu_2 \lambda_2 k_1^2 I H_o^{(1)}(\lambda_2 r)}{2\pi r_1 \mu_1 \sigma_1 k_2^2 H_1^{(1)}(\lambda_2 r_1)} \quad , \tag{26}$$

$$E_\theta^{(2)} = \frac{-i\mu_2 k_1^2 I\, H_1^{(1)}(\lambda_2 r)}{2\pi r_1 \omega\mu_1\sigma_1\, H_1^{(1)}(\lambda_2 r_1)} \quad , \tag{27}$$

$$E_r^{(2)} = \frac{-i\mu_2 h_b k_1^2 I\, H_1^{(1)}(\lambda_2 r)}{2\pi r_1 \mu_1\sigma_1 k_2^2\, H_1^{(1)}(\lambda_2 r_1)} \quad . \tag{28}$$

For this problem one obtains the propagation constant h_b as the (principal wave) root of a simpler determinantal equation:

$$\frac{k_1^2 J_1(\lambda_1 r_1)}{\mu_1\lambda_1 J_o(\lambda_1 r_1)} = \frac{k_2^2 H_1^{(1)}(\lambda_2 r_1)}{\mu_2\lambda_2 H_o^{(1)}(\lambda_2 r_1)} \quad . \tag{29}$$

Equation (29) is easily solved for h_b by the method of Sommerfeld. For large but finite wire conductivity one may assume that (provided r_1 is not too small):

$$\lambda_1 \approx k_1 >> 1 \quad , \quad \frac{J_o(\lambda_1 r_1)}{J_1(\lambda_1 r_1)} \rightarrow +i \quad . \tag{30}$$

In the principal mode the propagation constant h_b differs but slightly from k_2, hence the small argument Hankel expansions are applicable:

$$H_o^{(1)}(\lambda_2 r_1) \sim \frac{2i}{\pi}\, \ln\left(\frac{\gamma\lambda_2 r_1}{2i}\right) \quad , \quad H_1^{(1)}(\lambda_2 r_1) \sim \frac{-2i}{\pi\lambda_2 r_1} \quad . \tag{31}$$

The constant γ in (30) is $\sim$1.781.

Employing (31) and defining new variables

$$\xi = \left(\frac{\gamma\lambda_2 r_1}{2i}\right)^2 \quad , \quad \eta = \frac{-i\gamma^2}{2}\, \frac{\mu_1}{\mu_2}\, \frac{k_2^2 r_1}{k_1} \quad , \tag{32}$$

equation (29) may be solved by the iterative scheme

$$\xi_{n+1}\, \ln \xi_n = \eta \ , \quad \ln \xi_o \sim -20 \ . \tag{33}$$

The algorithm (33) is rapidly convergent. From the final iterate of ξ one may then solve the first equation of (32) for h_b. Numerically the above scheme may be slightly improved by explicitly evaluating the Bessel ratio in (30) for $|k_1 r_1| \leq 100$.

The MG Procedure

As a basis for extension to the insulated sheath model, Marston and Graham identify the bare wire situation of Figure 4 with the transmission line analog shown below in Figure 5:

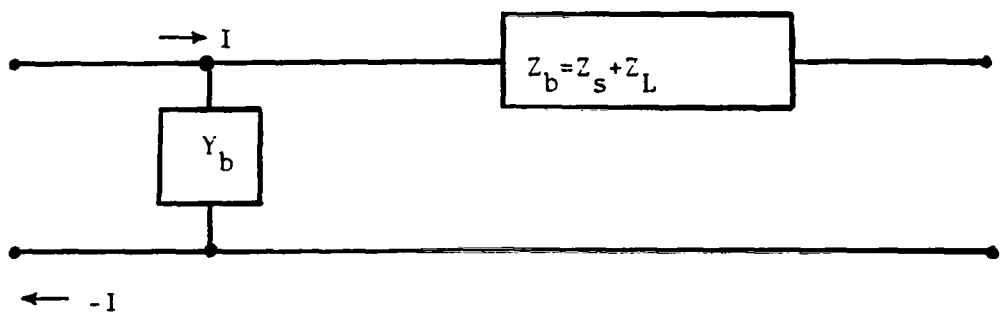

Figure 5. Bare Wire Transmission Line Section

It is essential that we discuss this analog in considerable detail.

In Figure 5, the total longitudinal impedance Z_b (with per unit length understood as before) is the series sum of the internal a.c. impedance of the wire (Z_s) and the lumped representation of the external impedance (Z_L). Y_b is the transverse admittance from the surface of the wire through the infinite outer dielectric medium.

We shall calculate impedances from the fields (26), (27), and (28). The "skin" impedance is:

$$Z_s = \frac{E_z(r=r_1)}{I} = \frac{\mu_2 \omega k_1^2 H_0^{(1)}(\lambda_2 r_1)}{2\pi r_1 \mu_1 \sigma_1 k_2^2 H_1^{(1)}(\lambda_2 r_1)} \approx \frac{(1-i)}{2\pi r_1}\sqrt{\frac{\mu_1 \omega}{2\sigma_1}} \quad . \tag{34}$$

The familiar approximate form of Z_s follows from (29), (30) and $k_1 \sim \sqrt{i\mu_1\sigma_1\omega}$. By the definition of inductance one notes that

$$Z_L = -i\omega L \ , \ L = I^{-1}\int_{r_1}^{\infty} B_\theta^{(2)}(r)dr \quad . \tag{35}$$

utilizing

$$\int_{r_1}^{\infty} H_1^{(1)}(\lambda_2 r)dr = \frac{H_o^{(1)}(\lambda_2 r_1)}{\lambda_2} \tag{36}$$

for the evaluation of (35) there results:

$$Z_L = \frac{-i\mu_2 k_1^2 H_o^{(1)}(\lambda_2 r_1)}{2\pi r_1 \sigma_1 \mu_1 \lambda_2 H_1^{(1)}(\lambda_2 r_1)} \approx \frac{i\omega\mu_2}{2\pi} \ \ln\left(\frac{\gamma\lambda_2 r_1}{2i}\right) \quad . \tag{37}$$

Small argument expansions (31) yield the approximate form of Z_L.

By direct addition of the exact expressions (34) and (37) we obtain:

$$Z_b = \frac{h_b^2}{k_2^2} Z_L \tag{38}$$

The expression (38) will prove useful in later discussion. Of course we expect Z_b to be dominated by Z_L as (38) clearly shows since $h_b \approx k_2$.

Having presented the impedance calculation "piecewise" let us now directly obtain the transmission line parameters for the bare wire. The transverse voltage at any point along the line is

$$V = \int_{r_1}^{\infty} E_r^{(2)}(r)dr = \frac{-i\mu_2 h_L k_1^2 I_o H_o^{(1)}(\lambda_2 r_1) e^{ih_L z} \ i\omega t}{2\pi r_1 \mu_1 \sigma_1 k_2^2 \lambda_2 H_1^{(1)}(\lambda_2 r_1)} \quad . \tag{39}$$

By definition we require that:

$$\frac{\partial V}{\partial z} = -Z_b I \tag{40}$$

From (39), solving for Z_b in (40) and comparing Z_L in (37) one may immediately obtain the previous expression (38). The remaining transmission line equation is

$$\frac{\partial I}{\partial z} = -Y_b V \quad . \tag{41}$$

Solving (41) for Y_b by again using (39) one finds:

$$Y_b = \frac{2\pi r_1 \sigma_1 \mu_1 \lambda_2 k_2^2 H_1^{(1)}(\lambda_2 r_1)}{\mu_2 k_1^2 H_0^{(1)}(\lambda_2 r_1)} \approx \frac{-2\pi(\sigma_2 - i\varepsilon_2 \omega)}{\ln\left(\frac{\gamma\lambda_2 r_1}{2i}\right)} \quad . \tag{42}$$

Note that from either the exact or the approximate expressions one may easily verify that $Z_b Y_b = -h_b^2$. The above derivation is equivalent to the original MG analysis of the bare wire. With due regard to (their) $e^{+i\omega t}$ convention, the results are identical.

In terms of the bare wire transmission line parameters let us first state the entire MG prescription for the coaxial line approximation, then recall the underlying assumptions. Denoting correspondence to the quantities of Section 3 by the sub-label "coax", the MG model is:

$$Z_{coax} \approx Z_b (\text{from (38)}) \quad , \tag{43}$$

$$Y_{coax} = \frac{Y_{sheath}\, Y_{soil}}{Y_{sheath} + Y_{soil}} \quad , \tag{44}$$

where,

$$Y_{soil} \approx Y_b (\text{from (42) with } r_1 \to r_1 + t) \tag{45}$$

t = sheath thickness = $r_2 - r_1$ of Section 3

and,

$$Y_{sheath} \approx \frac{2\pi(\sigma_2 - i\omega\varepsilon_2)}{\ln\left[\frac{r_1 + t}{r_1}\right]} \quad . \tag{46}$$

Propagation constant and characteristic impedance are therefore:

$$h_{coax} = \sqrt{-Z_{coax}\, Y_{coax}} \quad , \; I_m(h_{coax}) > 0 \; ; \tag{47}$$

$$(Z_c)_{coax} = \frac{-ih_{coax}}{Z_{coax}} \quad . \tag{48}$$

Bare wire quantities λ_2, h_b needed to calculate (43) and (45) are obtained by the Sommerfeld method applied to wires of radius r_1 and $r_1 + t$ respectively. Equations (43-48) and the former statement constitute a complete summary of the Marston-Graham buried cable approximation.

The assumption is made in (43) that the addition of a sheath to the bare wire will not appreciably alter the transmission line longitudinal impedance. The sheath will, however, have a blocking effect on the flow of transverse currents. One may therefore analyze the total transverse admittance through components as in (44) and Figure 2. In order to estimate the admittance through the soil (region 2 in this section) MG use the bare wire admittance (45) computed for a wire of radius equal to the outer sheath radius in the actual coaxial case. For the admittance through the sheath MG adapt (46), the well known expression for the admittance between two (coaxial) good conductors. Thus having specified Z and Y, the propagation constant and characteristic impedance may then be obtained through (47) and (48).

A Difficulty in the MG Model

Calculating the MG longitudinal impedance via (38) and (37) one immediately encounters a somewhat surprising result, namely that $Re(Z_L)$ and hence $Re(Z_b)$ are algebraically negative quantities. This result is evident in the original MG article upon examination of (their) equation (25) and Example II. The calculation of an apparently unphysical resistance naturally raises serious questions of interpretation.

Let us first demonstrate that the above mentioned result is indeed a consequence of the bare wire boundary value problem which was previously reviewed. Consistent with our propagation convention we must have:

$$\begin{aligned} k_2 &= a + ib \ , \ (a,b) > 0 \\ h_b &= \gamma + i\beta \ , \ (\gamma,\beta) > 0 \\ Im(\lambda_2^2 = k_2^2 - h_b^2) &= 2(ab - \gamma\beta) \ . \end{aligned} \tag{49}$$

Now as Sommerfeld first noted, the surrounding fields propagate into the wire and as a result, the waves suffer additional axial attenuation ($\beta > b$). The traveling waves exhibit also a slightly reduced phase velocity ($\gamma > a$). Clearly then from (49) one must find:

$$Im(\lambda_2^2) < 0 \ . \tag{50}$$

The bare wire fields (26-28) behave asymptotically (for large radii) as a Hankel function of the first kind with the form

$$\propto \frac{e^{+i(\lambda_2 r) - i\omega t}}{\sqrt{\lambda_2 r}} \ . \tag{51}$$

A self-contained physical system must have finite fields at infinity, hence from (51) only $Im(\lambda_2)>0$ is permissible. The restriction (50) then demands that λ_2 be of the form:

$$\lambda_2 = -c + id \ (c,d) > 0 \quad . \tag{52}$$

Consider now the approximate form of Z_L in (37). It is evident that given λ_2 of the form (52), the imaginary part of the logarithm argument is > 0 and hence $Re(Z_L) < 0$. We note that the foregoing is merely a simple way to reveal the sign of $Re(Z_L)$. The result is actually a consequence of (50) alone since one may express Z_L in terms of Z_s multiplied by a factor containing λ_2^2. Numerical evaluation of this alternate expression yields the same conclusion.

Fortunately the above "difficulty" has a simple and rather interesting interpretation. We shall demonstrate in the Appendix that the MG bare wire transmission line equations do indeed mathematically describe a well-known circuit analog, but one that is, however, <u>different</u> from that of Figure 5.

Having relegated further discussion of the bare wire circuit analog to the Appendix, let us attempt to clarify the use of Z_b in the Marston-Graham approximation. We need only to note that the MG assumption in (43) does not include an essential physical difference between the fields of the bare wire and those of the coaxial solution of section 3. Solving the coaxial model of the previous section we naturally demand $Im(\lambda_3)>0$ within the earth medium. We then find that λ_3 is of the form:

$$\lambda_3 = \sqrt{k_3^2 - h^2} = e + if \ (e,f) > 0 \ . \tag{53}$$

The result (53) occurs so long as the sheath conductivity has no dominating influence; such is the case of interest in this paper.

Since (e) in (53) is a positive number, we therefore obtain <u>outgoing</u> waves at asymptotic radii. By way of comparison to the "earth" medium in the bare wire situation, we have shown (52) that $Re(\lambda_{earth}) < 0$, representing <u>incoming</u> waves at asymptotic radii via (51). One will recall the familiar textbook example (reference 10) of Poynting's Theorem applied to an imperfectly conducting wire carrying current. The radial Poynting vector is directed inward (in the direction of radial propagation) and energy flows into the wire from the surrounding fields in amount equal to heat energy dissipated in the wire.

We therefore propose an obvious amendment to the original MG prescription. Let us agree to compute λ_2 (or λ_2^2) by the Sommerfeld method and having obtained the result (52), make the following <u>ad hoc</u> change:

$$\lambda_2 \text{ as in (52)} \rightarrow |c| + id$$

$$\text{equivalently, } \lambda_2^2 \rightarrow (\lambda_2^2)^* \quad . \tag{54}$$

The modified values (54) are to be employed in the calculation of <u>both</u> Z_b and Y_{soil} in (43) and (45) respectively. Note that (54) has only the effect on Z_b of changing the sign of $Re(Z_b)$; component magnitudes of Z_b do not change. The effect of (54) on Y_{soil} is also quite favorable. We shall discuss the latter point more fully in the next section.

The modification (54) simply reverses the direction of (asymptotic) radial propagation in the bare wire situation in order to achieve a closer physical approximation to the field structure of the coaxial case. In this regard, the addition of a sheath to the bare wire has an important (though indirect) effect on the estimation of the transmission line longitudinal impedance. Our arguments apply only to an essentially <u>insulating</u> sheath

for which (53) obtains. The model of section 3 yields results qualitatively no different from the bare wire model if the sheath medium is assigned a high enough conductivity.

5. NUMERICAL COMPARISON

We compare both real and imaginary parts of h, Z_c, Z and Y for the coaxial transmission line as obtained from both the field analysis of Section 3 and from the Marston-Graham model of Section 4. Figures 6 through 29 present the comparative results (log-log plots) for three distinct cases as indicated. Negative quantities are graphically indicated by arrowheads superimposed on a plotted line. The individual cases will be discussed sequentially for clarity.

Cable geometry is that of Figure 3. Common to all three cases we have taken:

$$\mu_1 = \mu_2 = \mu_3 = 4\pi \times 10^{-7} \text{ henry/meter}$$

$$\sigma_1 = 5.8 \times 10^7 \text{ mhos/meter (copper)}$$

$$\sigma_3 = 10^{-3} \text{mhos/meter (earth medium)}$$

$$\varepsilon_3 = 10\varepsilon_o \ , \ \varepsilon_o = \frac{1}{36\pi} \times 10^{-9} \text{ farad/meter.}$$

<u>Case 1</u>

Results are displayed in Figures (6-13). The remaining cable parameters are:

$$r_1 = .9 \times .0254 \text{ meters} \qquad r_2 = (.9+.065) \times .0254 \text{ meters}$$

$$\varepsilon_2 = 2.75\ \varepsilon_o \text{ (sheath medium)} \ , \ \sigma_2 = 0.$$

The Marston-Graham quantities are labeled MG on the graphs. For this case, we show the consequences of the original MG prescription as discussed in the previous section. The MG longitudinal resistance (Figure 10) is negative and this unphysical result introduces serious discrepancy into the comparison with the model of Section 3. Most notable is the effect on the line attenuation constant (Figure 7) and on Im (Z_c) evident in Figure 9. Observe that the MG admittance (Figures 12 and 13) has no radical departure from the other model up to frequencies $\sim 5 \times 10^6$ Hertz. Over this frequency range we see that the actual (asymptotic) direction of radial propagation in the bare wire solution is not a critical factor in the MG admittance assumptions.

Case 2

All parameters have the identical values of Case 1. For this example we consider the modified MG model resulting from the plausibility arguments leading to (54) in Section 4. The results are presented in Figures (14-21). For frequencies $\lesssim 10^7$ Hertz the MG model now yields a reasonable propagation constant (Figures 14 and 15) and characteristic impedance (Figures 16 and 17). As we earlier pointed out, only the sign of Re(Z) in Figure 18 changes in comparison to Case 1.

It is important to note that the modification (54) improves also the MG admittance estimations (Figures 20 and 21). Most significant is the MG prediction of similar high frequency behavior in the transverse conductance (Figure 20). The latter behavior will be discussed at the end of this section.

While agreement is certainly not quantitative, the overall qualitative agreement is excellent. The Marston-Graham approach can thus apparently be made to contain most of the essential physics of the extended coaxial situation considered in this paper. The modified MG model should be quite adequate for rough calculations. For more quantitatively critical cable current predictions, one should employ the model of section 3, if possible.

Case 3

Cable parameters are:

$r_1 = 1.19 \times .0254$ meters $\qquad r_2 = (1.19 + .1) \times .0254$ meters

$\varepsilon_2 = 2.26\varepsilon_0$ $\qquad \sigma_2 = 10^{-8}$ mhos/meter .

Results for this final example are displayed in Figures (22-29). As in the previous case, we employ the modified Marston-Graham model.

The comments regarding the Case 2 comparison apply equally well to this example. Note especially the additional (over that of previous results) structure in $\mathrm{Im}(Z_c)$; the MG model again can qualitatively reproduce the detailed behavior of the model in section 3.

The Transverse Conductance

Upon implementing the scheme outlined in Section 3, we find (for the test case parameters above) that at frequencies $\gtrsim 10^7$ Hertz, the calculated transverse conductance becomes negative. From a practical standpoint, this unfortunate behavior is actually of little consequence, as we shall elaborate momentarily. The result is puzzling, but in this

paper we offer no definitive explanation. We can, however, make some pertinent observations.

We believe that our solution to the three-medium determinantal equation is correct. The roots h were obtained smoothly as a function of frequency step-wise through fine increments. Our solutions for h compare well with those of Price and Stevenson (reference 2). As did the former authors, we have located non-principal wave roots, but find the real parts to have magnitudes $\gtrsim 100$ times that of the desired solutions. It appears that the admittance anomaly is a theoretical limitation of the model itself. The fact that the modified Marston-Graham procedure predicts the same behavior tends to support such a conclusion.

At frequencies $\gtrsim 10^7$ Hertz our test cases show that waves on the line would be almost totally damped within a distance of ~500 meters. Thus typical current calculations on long cables cannot be appreciably affected by the region of anomalous admittance.

The admittance difficulty is strongly dependent on the assumed conductivity of the earth medium. We find, for example, that with $\sigma_3 = 1$ mhos/meter (and other parameters similar to our test cases), Re(Y) stays positive for frequencies $\lesssim 10^{10}$ Hertz.

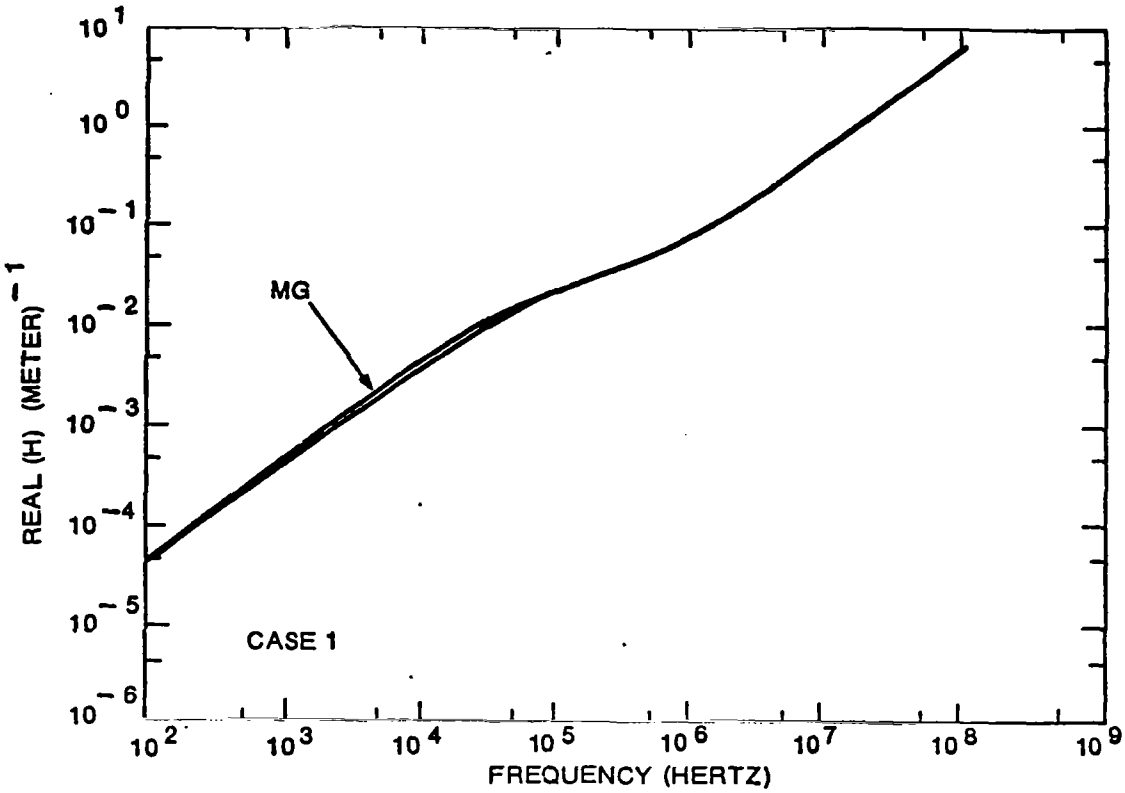

Figure 6. Real Parts of Propagation Constant Versus Frequency

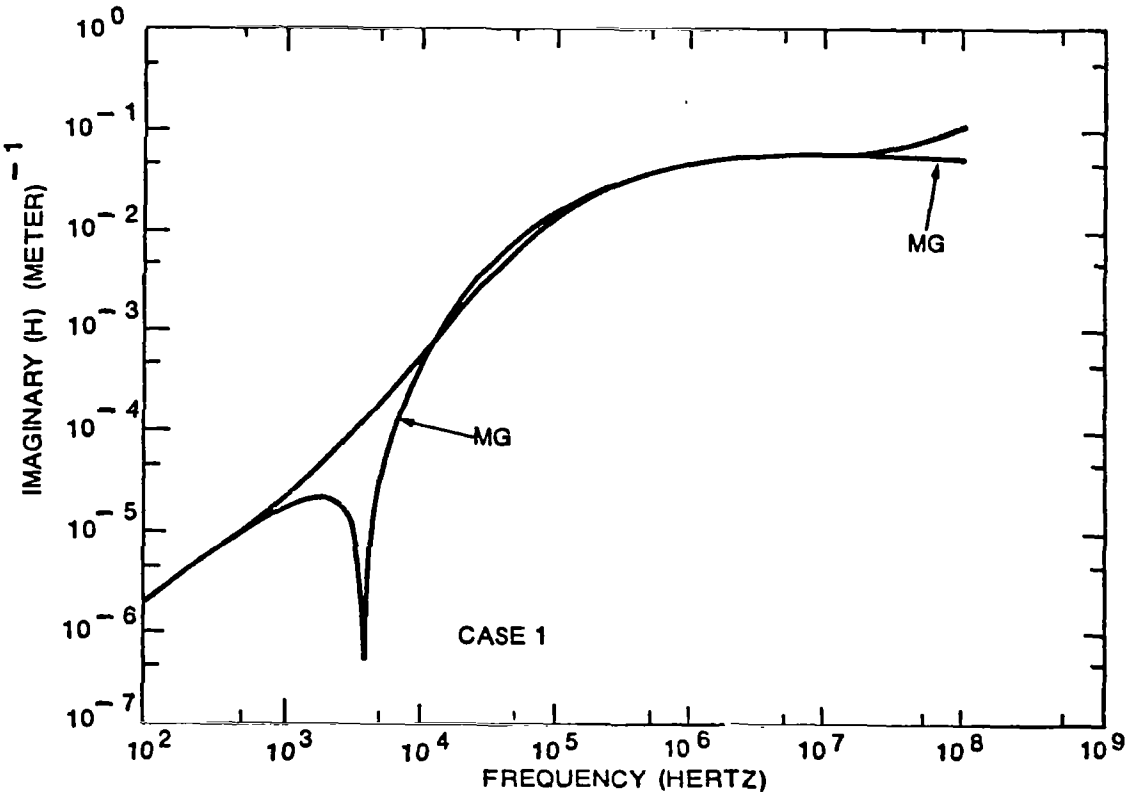

Figure 7. Imaginary Part of Propagation Constant Versus Frequency

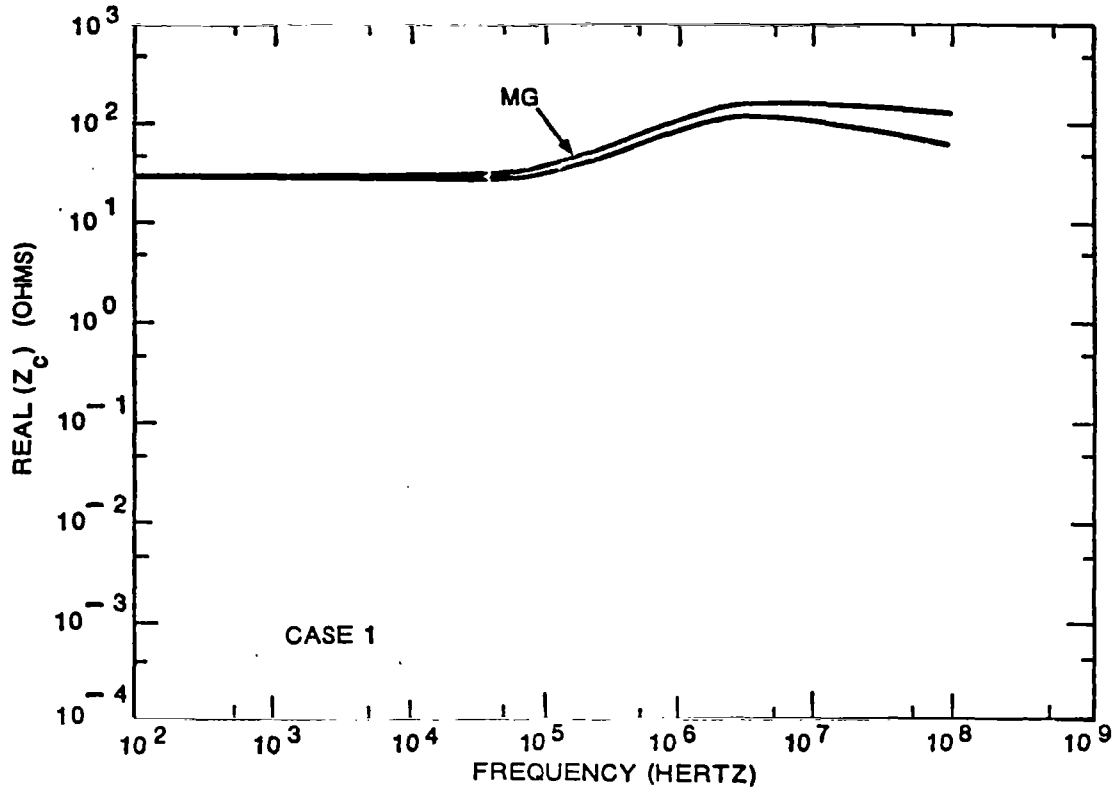

Figure 8. Real Part of Characteristic Impedance Versus Frequency

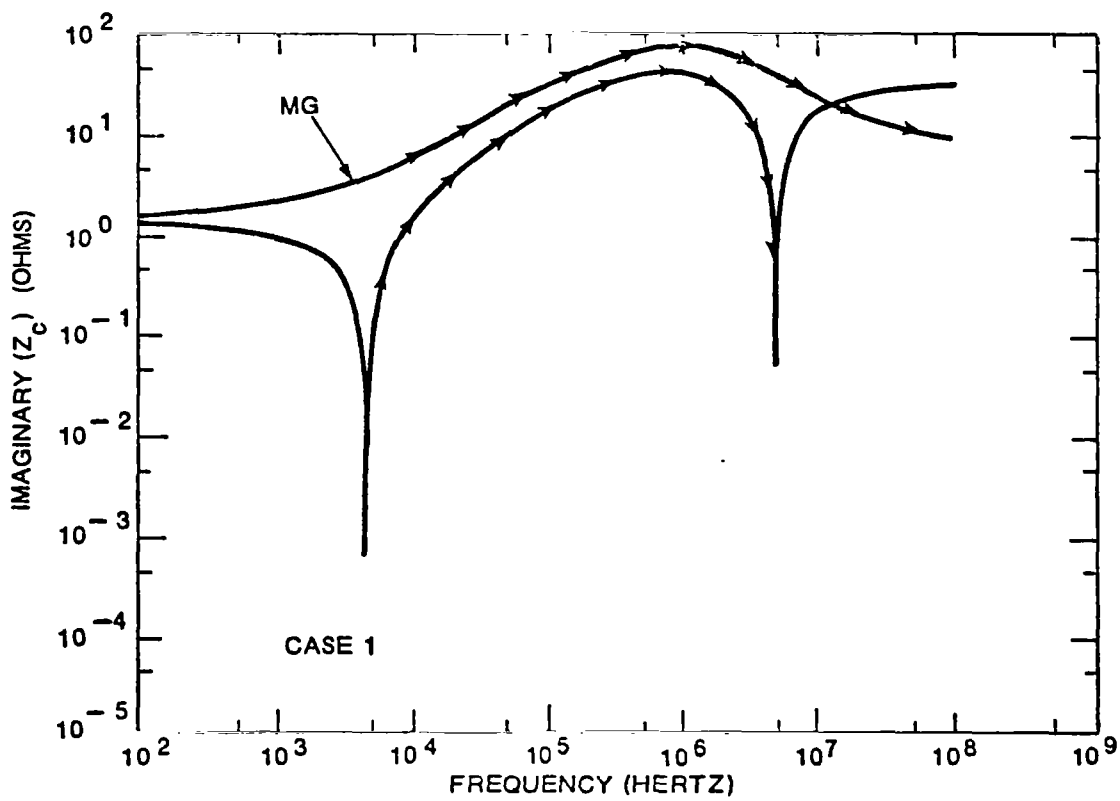

Figure 9. Imaginary Part of Characteristic Impedance Versus Frequency

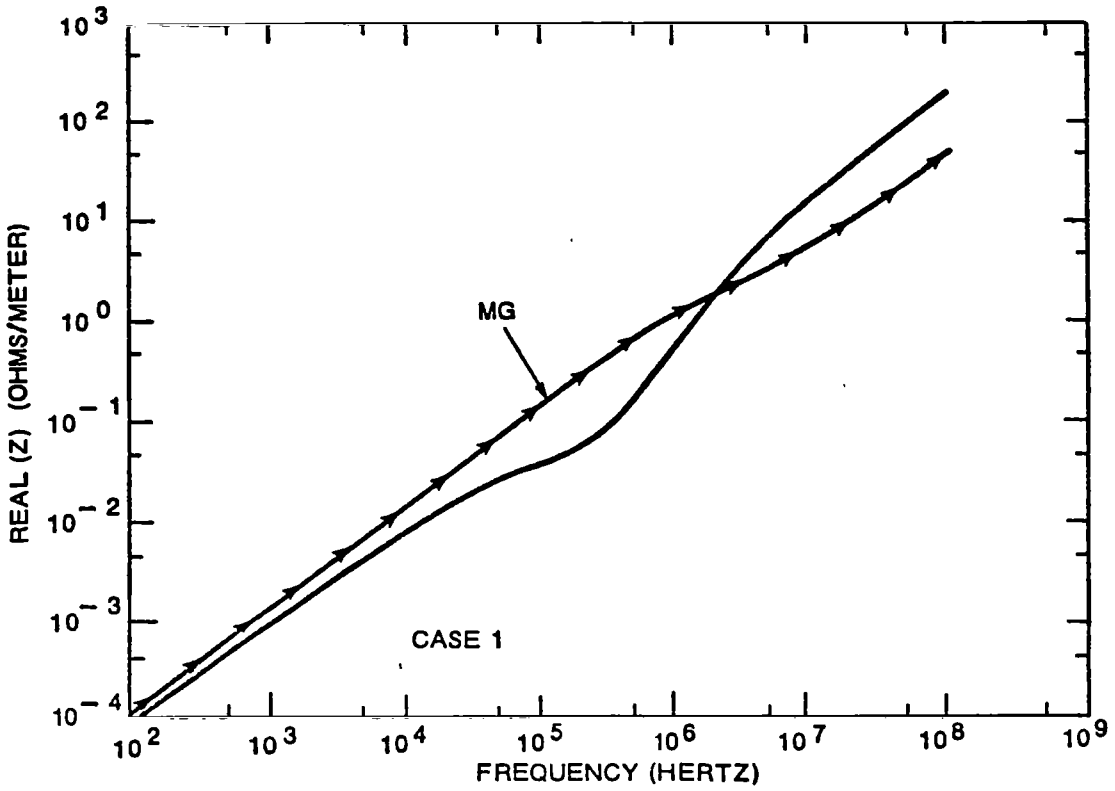

Figure 10. Real Part of Longitudinal Impedance Versus Frequency

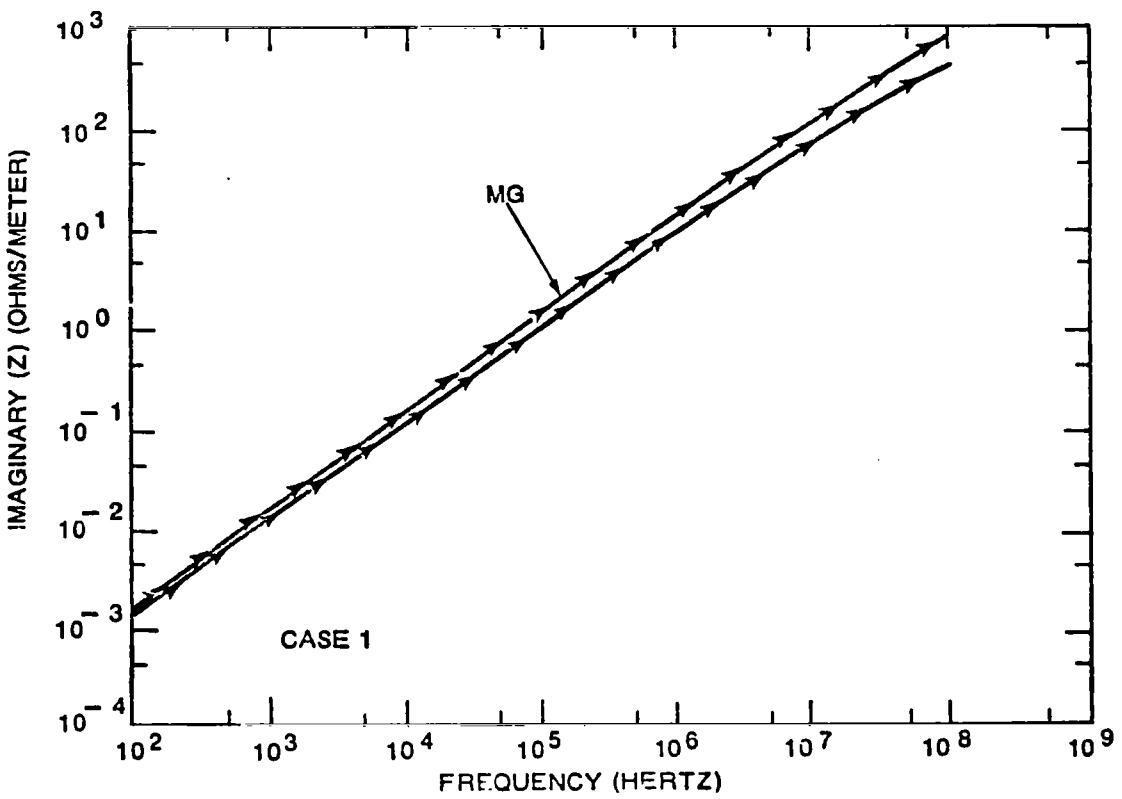

Figure 11. Imaginary Part of Longitudinal Impedance Versus Frequency

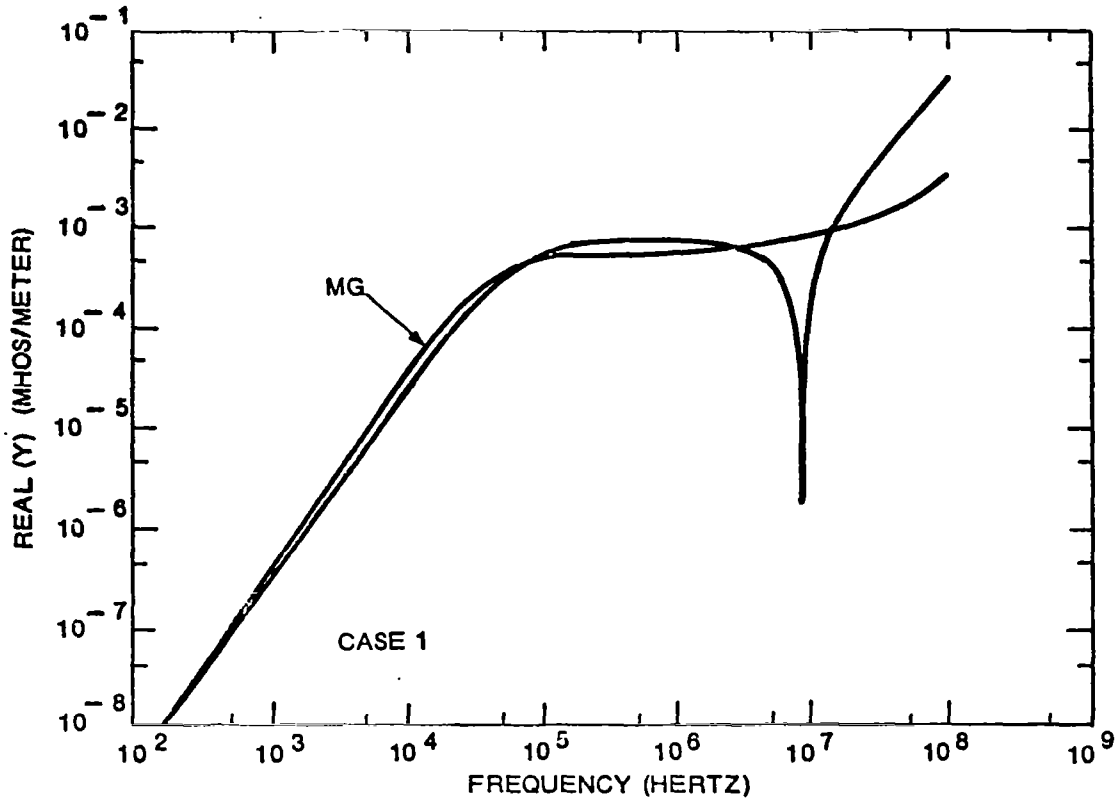

Figure 12. Real Part of Transverse Admittance Versus Frequency

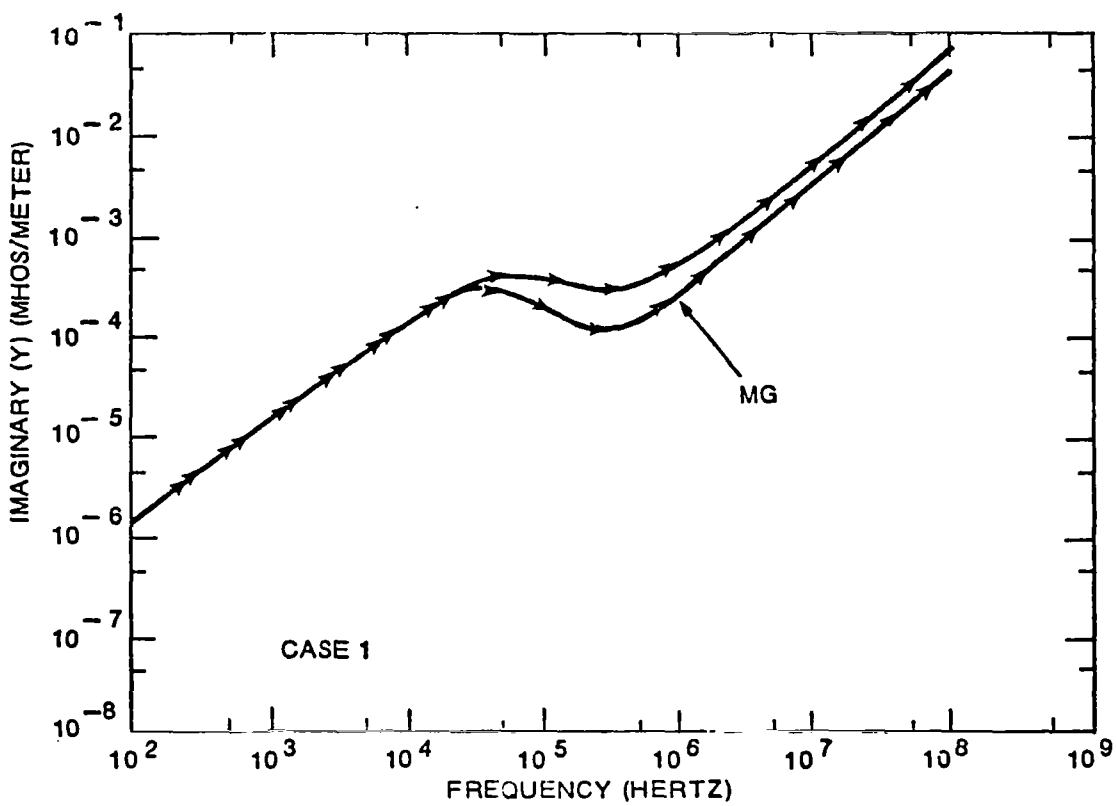

Figure 13. Imaginary Part of Transverse Admittance Versus Frequency

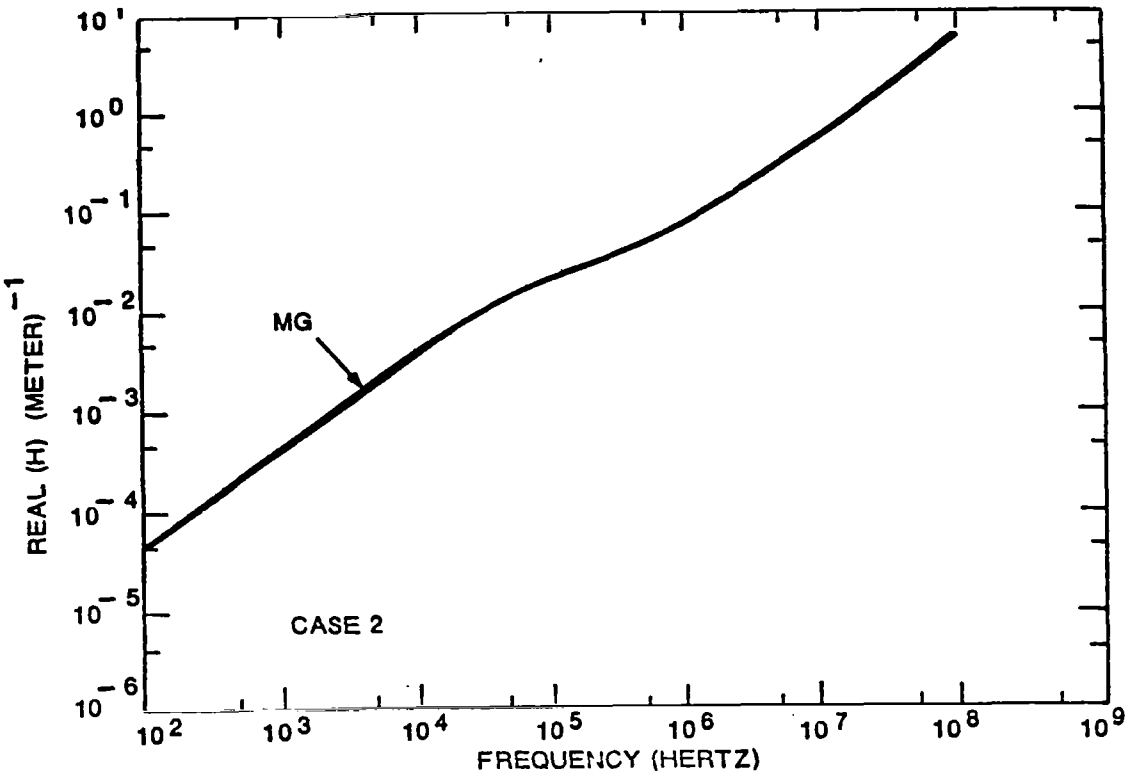

Figure 14. Real Part of Propagation Constant Versus Frequency

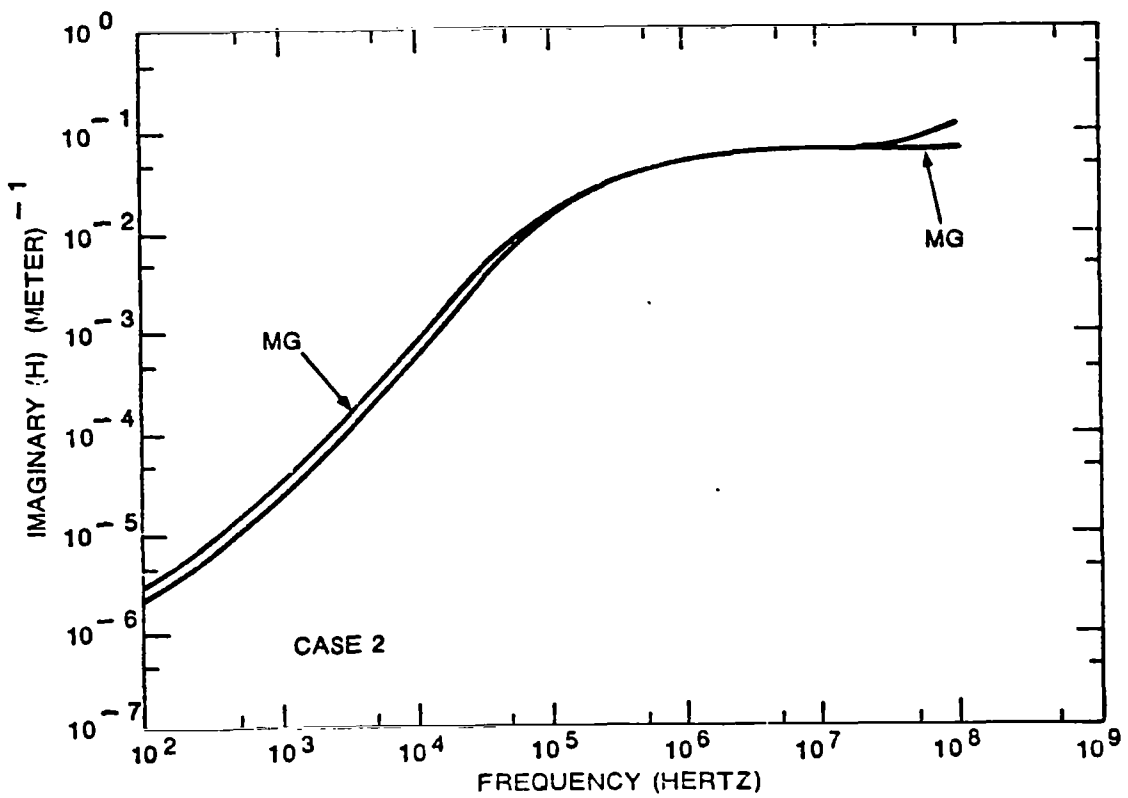

Figure 15. Imaginary Part of Propagation Constant Versus Frequency

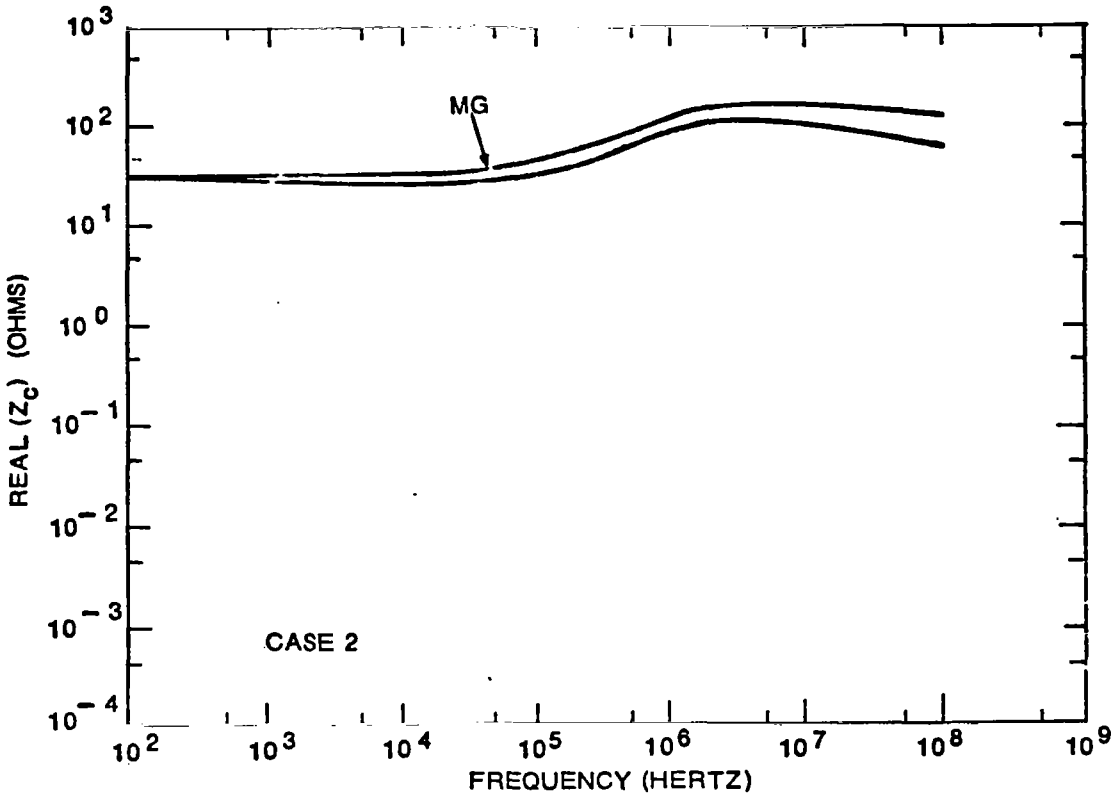

Figure 16. Real Part of Characteristic Impedance Versus Frequency

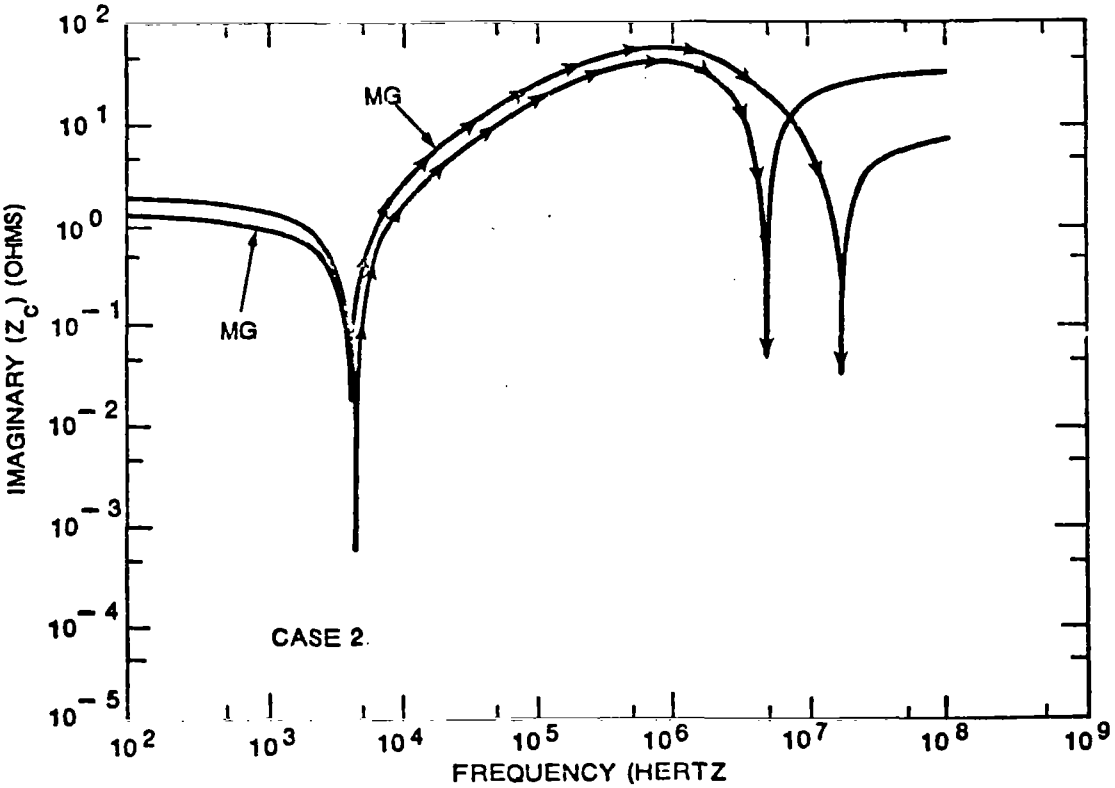

Figure 17. Imaginary Part of Characteristic Impedance Versus Frequency

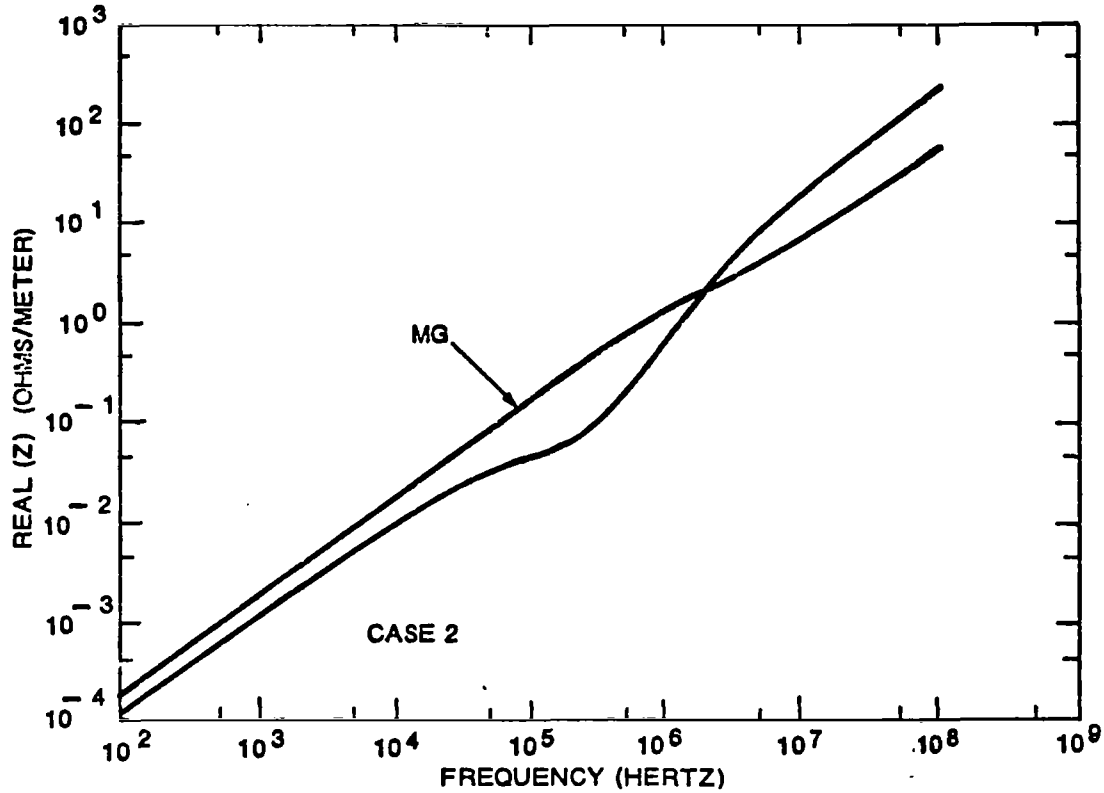

Figure 18. Real Part of Longitudinal Impedance Versus Frequency

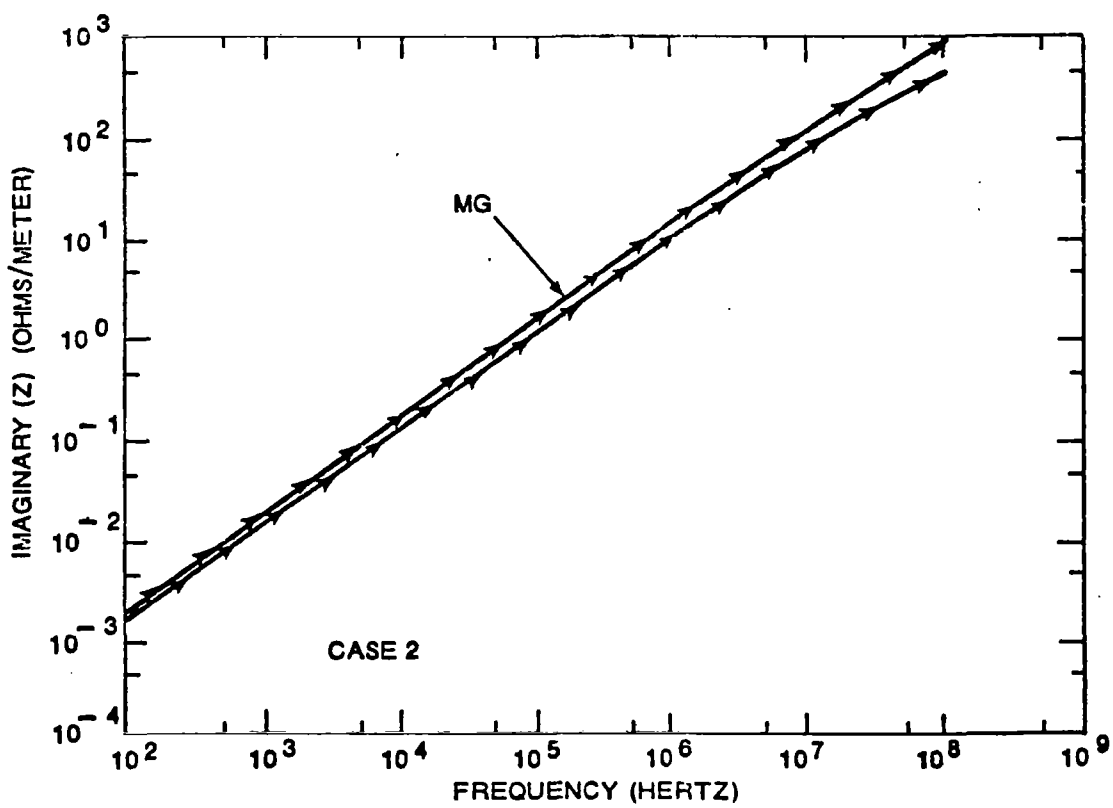

Figure 19. Imaginary Part of Longitudinal Impedance Versus Frequency

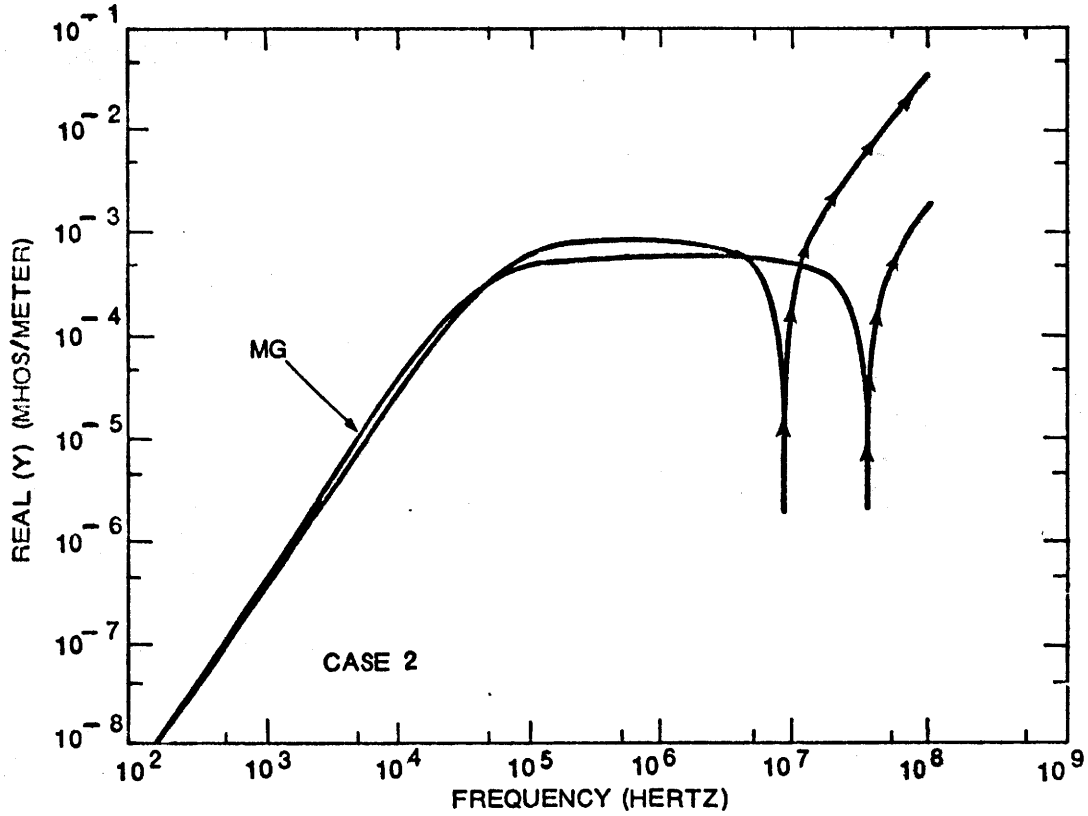

Figure 20. Real Part of Transverse Admittance Versus Frequency

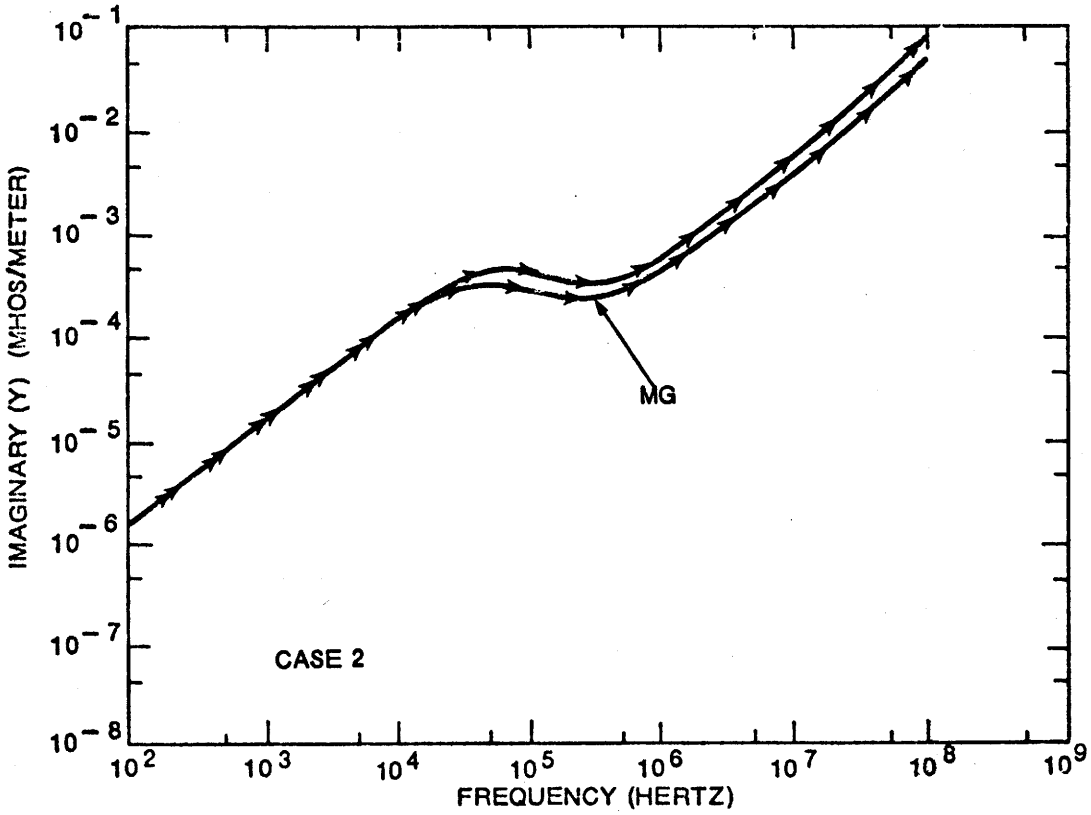

Figure 21. Imaginary Part of Transverse Admittance Versus Frequency

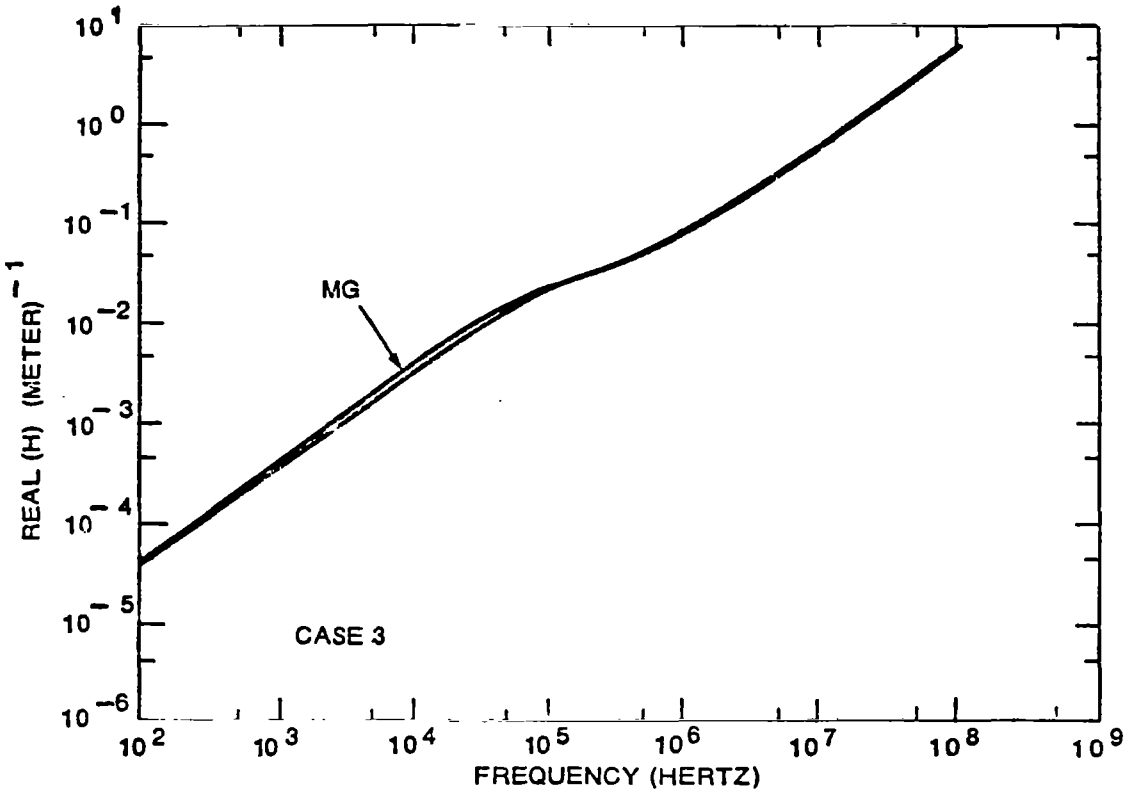

Figure 22. Real Part of Propagation Constant Versus Frequency

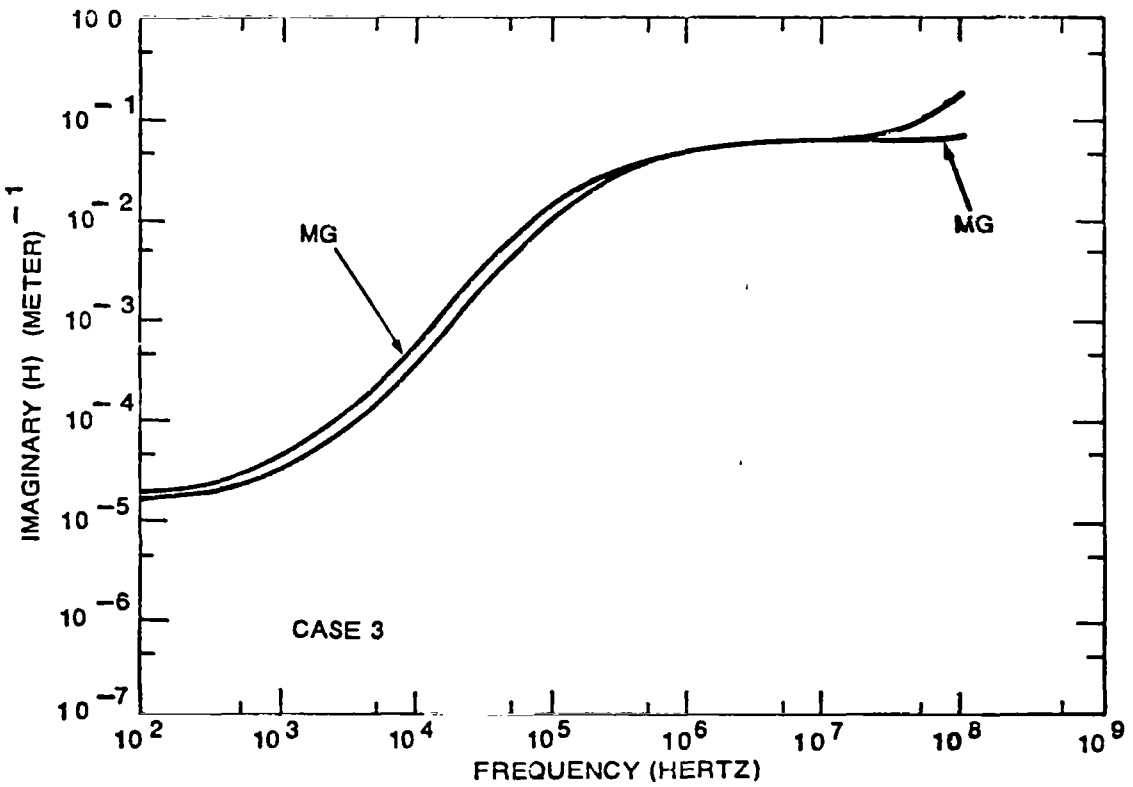

Figure 23. Imaginary Part of Propagation Constant Versus Frequency

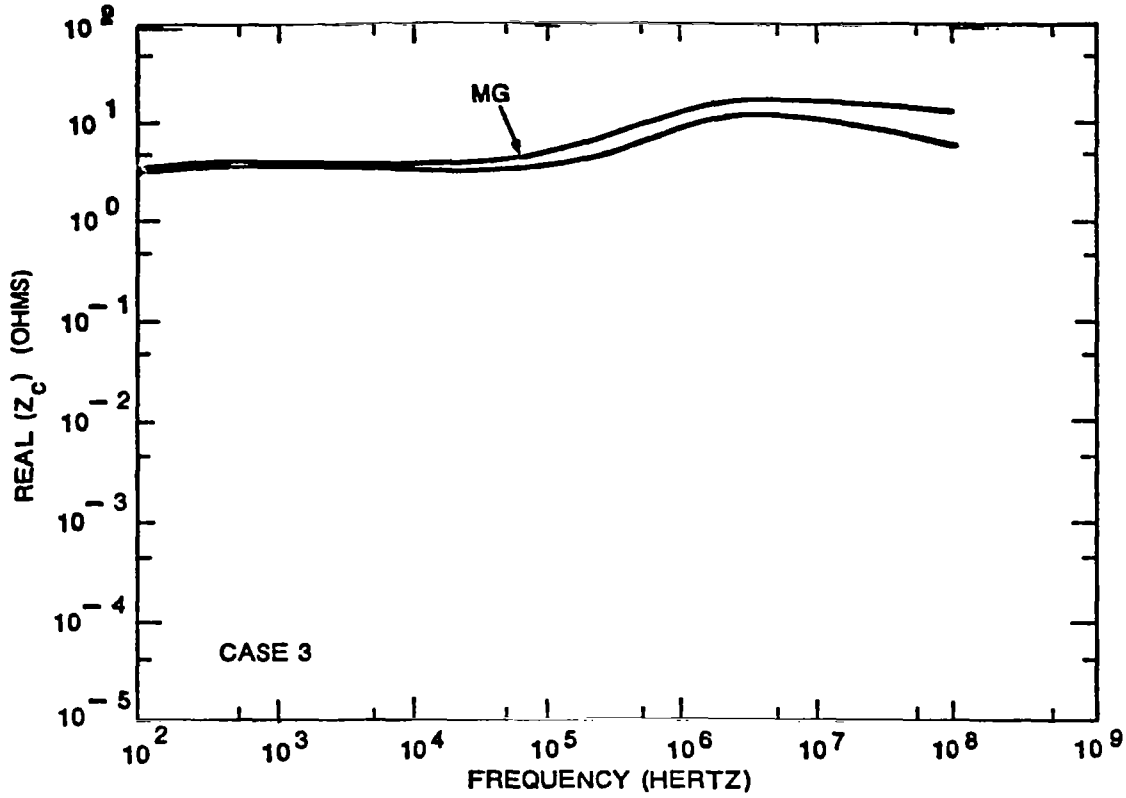

Figure 24. Real Part of Characteristic Impedance Versus Frequency

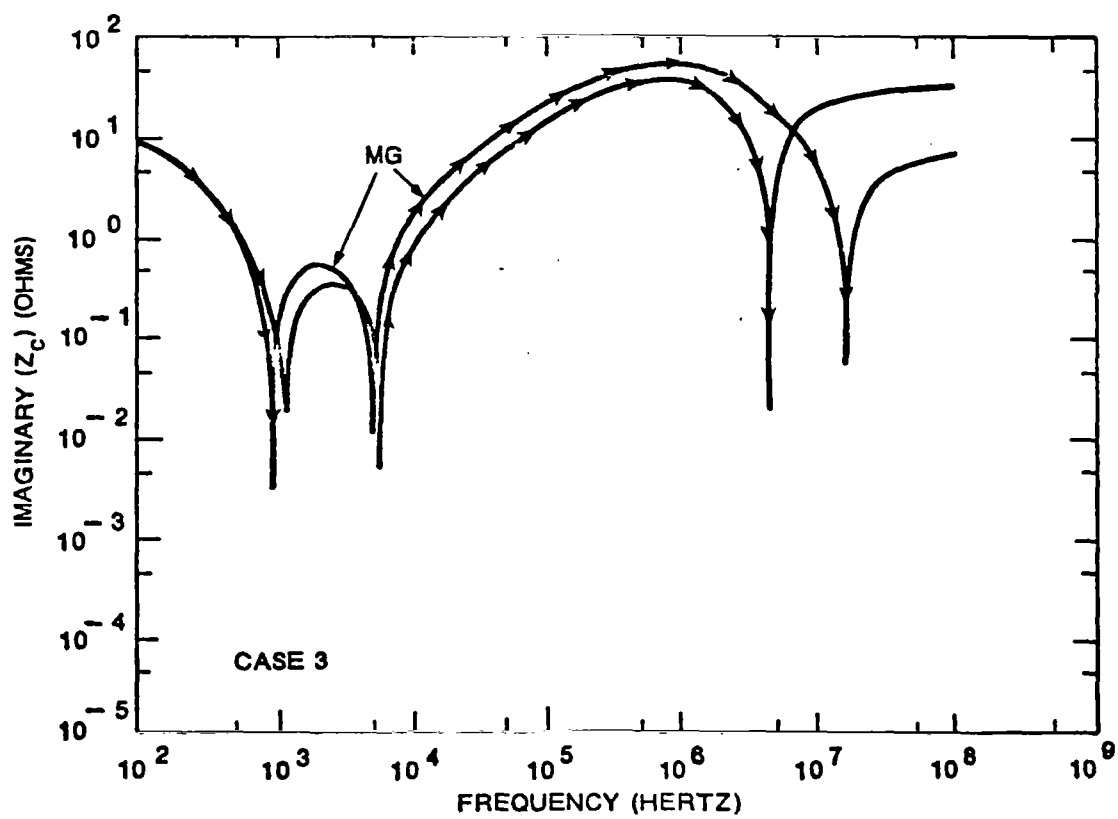

Figure 25. Imaginary Part of Characteristic Impedance Versus Frequency

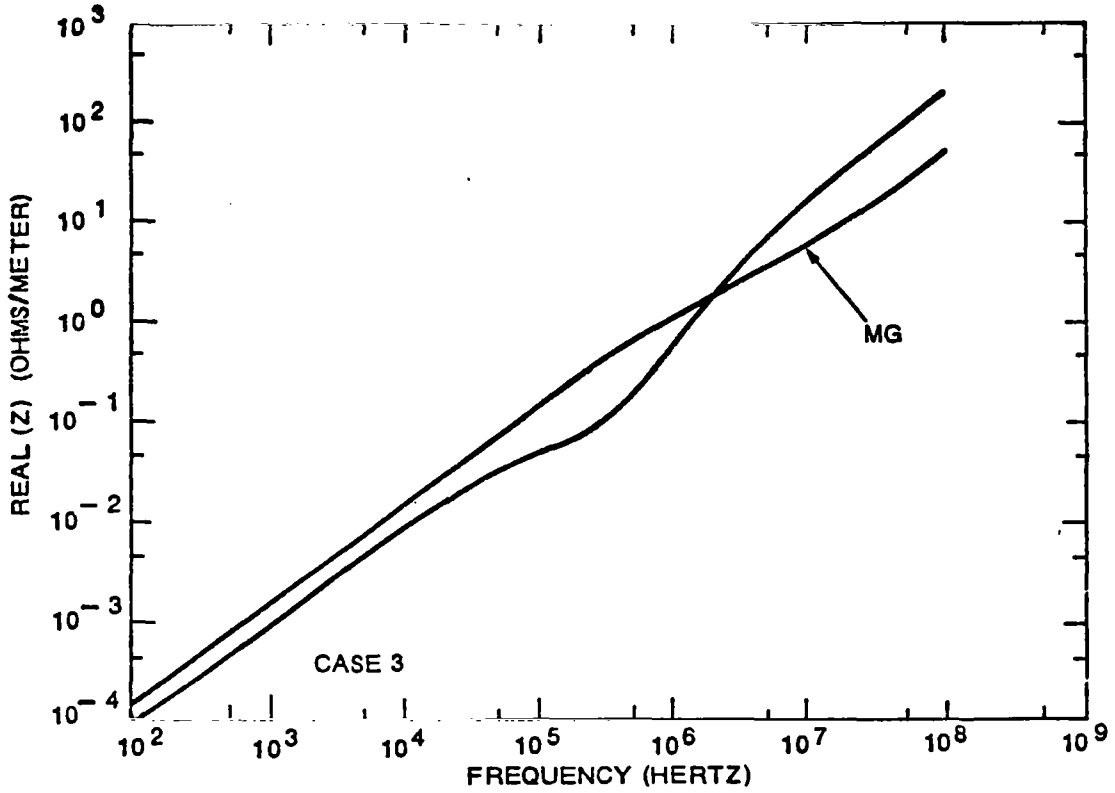

Figure 26. Real Part of Longitudinal Impedance Versus Frequency

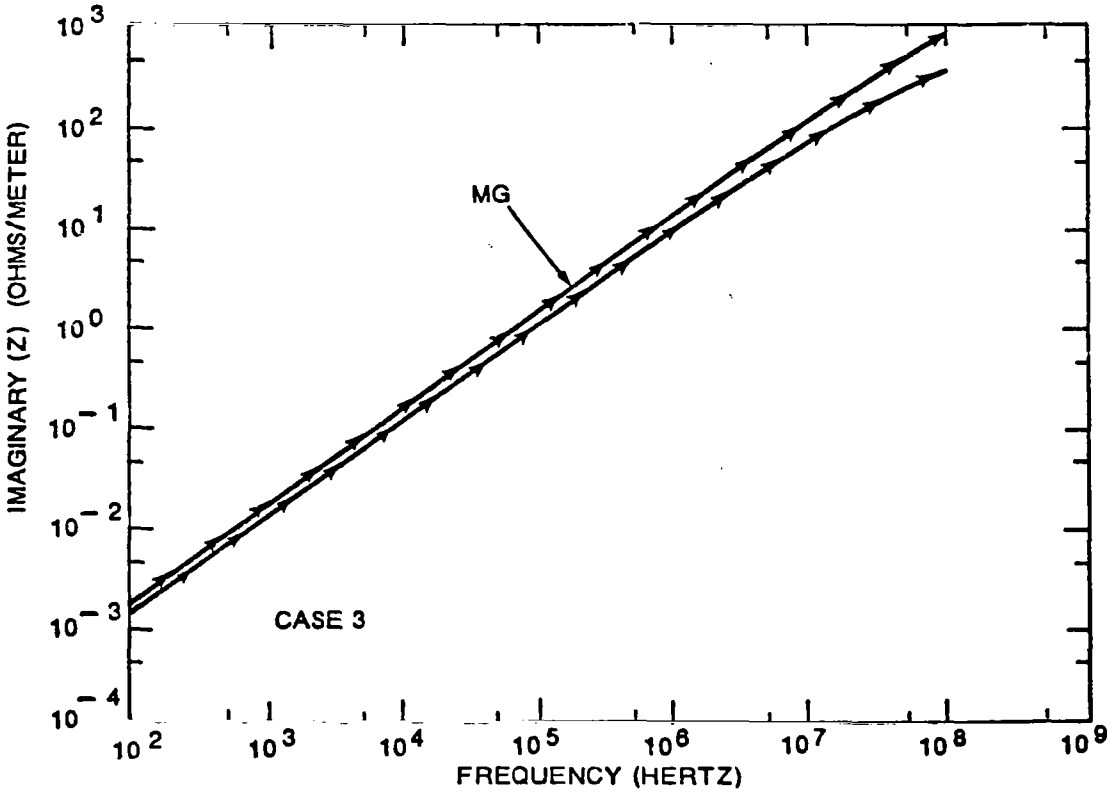

Figure 27. Imaginary Part of Longitudinal Impedance Versus Frequency

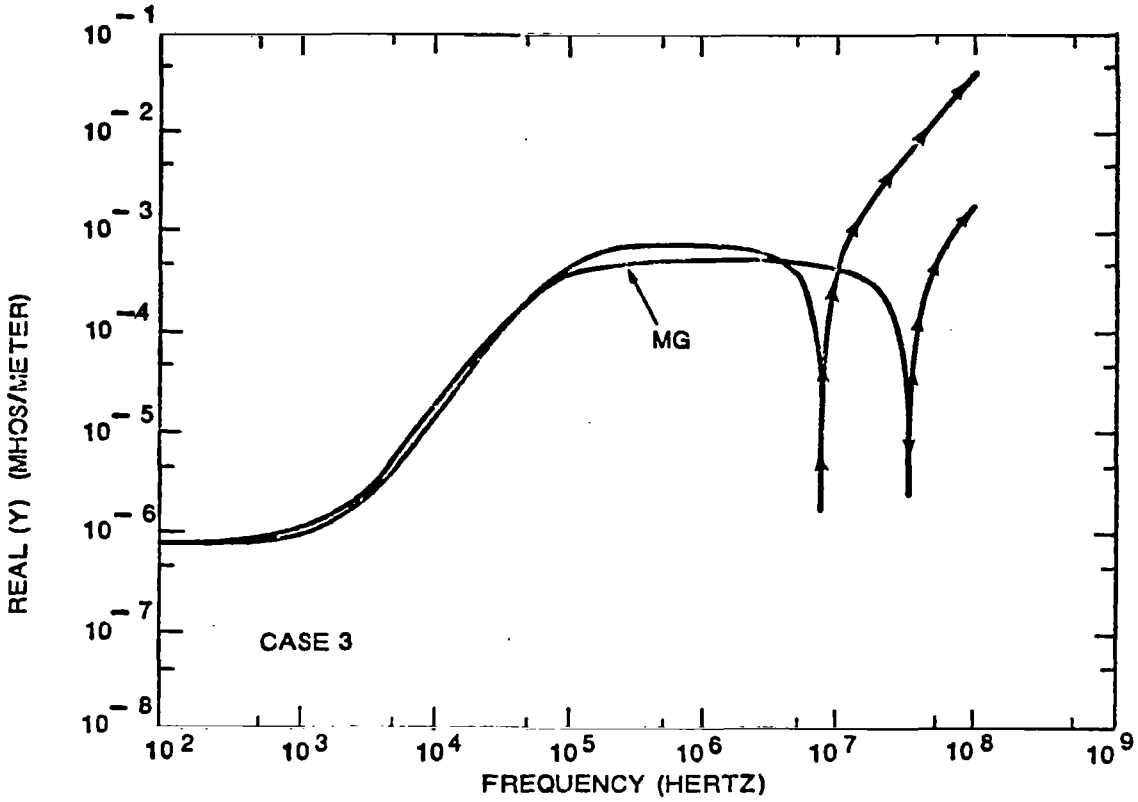

Figure 28. Real Part of Transverse Admittance Versus Frequency

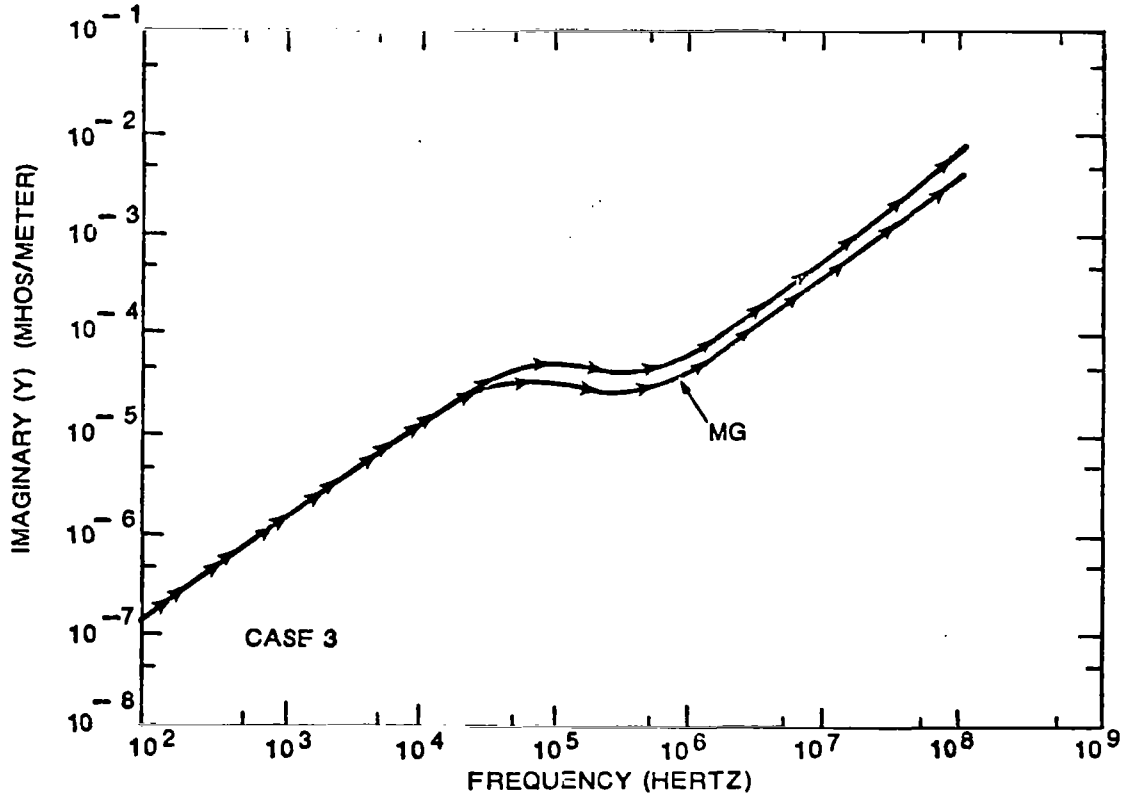

Figure 29. Imaginary Part of Transverse Admittance Versus Frequency

6. CONCLUSIONS

In this paper we have considered an idealized buried cable: an insulated infinitely long wire embedded in a homogeneous, lossy dielectric "earth" medium of infinite extent. Transmission line parameters were defined and calculated from the free oscillation field analysis of the sheathed wire.

Using the former calculation as a bench mark we compared the line parameters resulting from the Marston-Graham approach. The original MG assumption for the estimation of the longitudinal impedance led to a model precluding any reasonable correspondence. A physically plausible reinterpretation of (their) assumption was then shown to yield a model in detailed qualitative agreement with the predictions of the three-medium normal mode approach.

One would reasonably apply the models we have discussed only to current predictions on long cables. The high frequency transverse conductance anomalies evident in both models can then be safely ignored. We finally conclude that for quantitative cable calculations, it would be clearly desirable to utilize the parameters of the more exact analysis, if at all possible. The modified MG model should, however, be quite suitable for engineering estimates.

APPENDIX

TRANSMISSION LINE CIRCUIT FOR THE BARE WIRE

In section 4, following Marston and Graham, we calculated (via a natural mode analysis) a transmission line longitudinal impedance Z_b for a bare wire embedded in an infinite dielectric. We showed that the unmodified adoption of Z_b as the impedance of a sheathed wire transmission line is physically unacceptable since the sign of $Re(Z_b)$ is negative. Unlike the sheathed wire model, however, the MG bare wire transmission line equations may be interpreted in terms of an equivalent circuit conceptually different from that of Figure 5 (and free of the former difficulty). Thus we shall demonstrate that for the bare wire, the "negative resistance" is actually only a matter of interpretation and not a patently unphysical result.

The alternate circuit we wish to examine is well-known to engineers, viz. the equivalent circuit representation of a transverse magnetic (TM) guided wave. It is evident that the Sommerfeld bare wire analysis may be viewed as the determination of the propagating modes of a TM waveguide. Let us therefore consider an axially symmetric TM wave propagating in an infinite, lossy dielectric medium characterized by $(\mu_2, \sigma_2, \varepsilon_2)$. The wave is guided along a finitely conducting wire of radius r_1. As throughout this paper, the assumed time dependence is $e^{-i\omega t}$.

We shall need only two of the appropriate Maxwell equations. From the curl $\vec{E}$ equation:

$$\frac{\partial E_r}{\partial z} - \frac{\partial E_z}{\partial r} = i\omega\mu_2 H_\theta \quad . \tag{1}$$

The curl $\vec{H}$ equation yields:

$$\frac{\partial H_\theta}{\partial z} = -(\sigma_2 - i\omega\varepsilon_2)E_r \quad . \tag{2}$$

Assuming a waveguide z dependence of $e^{ih_b z}$ one may solve (1) and (2) for H_θ:

$$H_\theta = \frac{-(\sigma_2 - i\omega\varepsilon_2)}{k_2^2 - h_b^2} \frac{\partial E_z}{\partial r} \quad . \tag{3}$$

Now $(\text{curl } \vec{E})_z = 0$, so in any transverse plane we may obtain the radial electric field from minus the gradient of a scalar potential V:

$$E_r = \frac{-\partial V}{\partial r} \quad . \tag{4}$$

Observe that we may combine (2) with (3) and (4):

$$\frac{\partial}{\partial z}\left[\frac{(\sigma_2 - i\omega\varepsilon_2)}{k_2^2 - h_b^2} \frac{\partial E_z}{\partial r}\right] = -(\sigma_2 - i\omega\varepsilon_2)\frac{\partial V}{\partial r} \quad . \tag{5}$$

Similarly, by combining (1), (3) and (4) we obtain

$$\frac{\partial}{\partial z}\left(\frac{\partial V}{\partial r}\right) = -\left[\frac{-h_b^2}{\sigma_2 - i\omega\varepsilon_2}\right]\left[\frac{\sigma_2 - i\omega\varepsilon_2}{k_2^2 - h_b^2} \frac{\partial E_z}{\partial r}\right] \quad . \tag{6}$$

The radial derivatives in (5) and (6) can be removed within a constant of integration which we are free to choose. For the bare wire situation, let us note that $E_z(r \to \infty) = 0$ and let us define the potential so

that $V(r \to \infty) = 0$. We may then integrate (5) and (6) by the following (suppressing radial dependence of V):

$$\int_{r_1}^{\infty} \frac{\partial V}{\partial r}\, dr = -V \;, \int_{r_1}^{\infty} \frac{\partial E_z}{\partial r}\, dr = -E_z(r=r_1) \tag{7}$$

The bare wire transmission line analog is the statement of (5) and (6) with (7). We identify the transmission line current:

$$I_z \equiv \frac{(\sigma_2 - i\omega\varepsilon_2)}{k_2^2 - h_b^2}\; E_z(r=r_1) \quad . \tag{8}$$

Transmission line equations are

$$\frac{\partial V}{\partial z} = -ZI_z \;, \tag{9}$$

and,

$$\frac{\partial I_z}{\partial z} = -YV \;. \tag{10}$$

The line parameters are just

$$Z = \frac{-h_b^2}{\sigma_2 - i\omega\varepsilon_2} = -i\omega\mu_2\left(\frac{h_b^2}{k_2^2}\right) \tag{11}$$

and

$$Y = \sigma_2 - i\omega\varepsilon_2 \quad . \tag{12}$$

Figure A-1 shows the equivalent circuit section for the transmission line of (8-12):

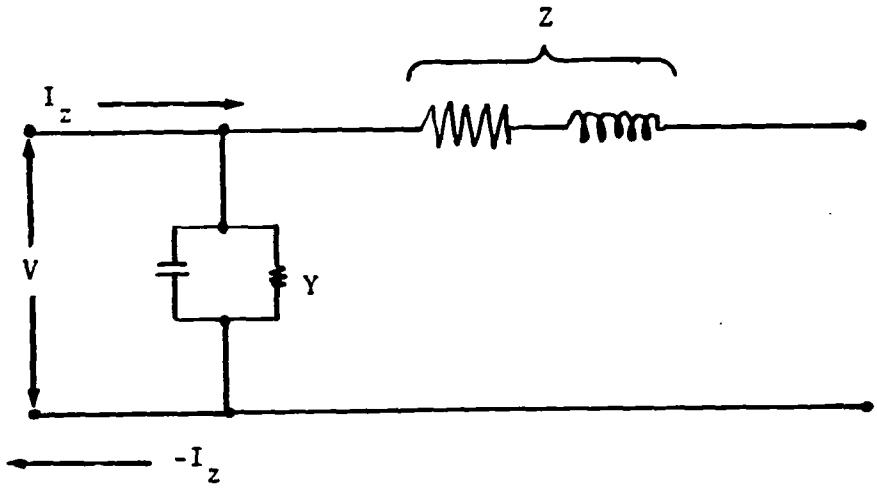

Figure A-1. Bare Wire TM Waveguide Equivalent Circuit

A discussion of guided wave transmission line analogs may be found in (reference 6).

The transverse voltage V in Figure A-1 is exactly the definition previously applied to the bare wire in section 4. The Sommerfeld solution again determines h_b. Note that since typically $h_b \approx k_2$ then from (11), $Z \approx -i\omega\mu_2$ and principally inductive. It is easy to demonstrate, using the previous (section 4) physical arguments given regarding h_b and k_2, that the small resistive part of (11) is in fact always positive.

The transmission line current I_z in (8) relates to conduction and displacement currents in the dielectric (the factor $\sigma_2 - i\omega\varepsilon_2$) and it relates to the current in the wire I_{wire} via the boundary condition on $E_z(r = r_1)$ at the guide surface. Denoting as before the a.c. impedance of the wire by Z_s, we have

$$E_z(r = r_1) \equiv Z_s I_{wire} \quad . \tag{13}$$

and from (8):

$$I_{wire} = \frac{(k_2^2 - h_b^2) I_z}{(\sigma_2 - i\omega\varepsilon_2) Z_s} \quad . \tag{14}$$

Suppose we wish to use our waveguide transmission line model for a practical current calculation given a driving field $E_d(z,\omega)$. Solving the driven transmission line equation (5) (infinite line) for $I_z(\omega,z)$ and using (14) we obtain:

$$I_{wire}(\omega,z) = \frac{i(k_2^2-h_b^2)}{2h_b Z_s}\int_0^\infty E_d(u,\omega)e^{ih_b|z-u|}du \quad . \tag{15}$$

Now consider the MG bare wire analog obtained by formal identification with the circuit of Figure 5. Recall from section 4 that we showed (38):

$$Z_b = \frac{h_b^2}{k_2^2} Z_L \ , \ Z_b = Z_s + Z_L \quad . \tag{16}$$

Eliminating Z_L in (16) one finds

$$Z_b = \frac{-h_b^2 Z_s}{k_2^2-h_b^2} \quad . \tag{17}$$

For the driven line current the MG model yields:

$$I_{wire}(\omega,z) = \frac{-ih_b}{2Z_b}\,(\text{space integral}) \equiv \frac{i(k_2^2-h_b^2)}{2h_b Z_s}\int_0^\infty E_d(u,\omega)e^{ih_b|z-u|}du \quad . \tag{18}$$

Thus with the aid of (17) we see that the MG bare wire transmission line equations are mathematically equivalent to those of the waveguide analog. The bare wire model need not, therefore, be interpreted on the basis of the circuit in Figure 5.

As evidenced in the "hybrid" current I_z it should be apparent that the unique features of the bare wire model arise from the fact that there is no physical separation between the wire current and the

current in the dielectric medium. Precisely such a separation is provided in the coaxial sheath model.

REFERENCES

1. Marston, D. R., Graham, W. R., "Currents Induced in Cables in the Earth by a CW Electromagnetic Field", 1966, Air Force Weapons Laboratory EMP Interaction Note No. 24, vol. 2

2. Price, H. J., Stevensen, D. E., "Notes on Planar, Cylindrical Electromagnetic Wave Propagation on Circularly-Symmetric Transmission Lines", 1969, Air Force Weapons Laboratory EMP Interaction Note No. 26, vol. 2

3. Head, J. H., "The Effects of the Air-Earth Interface on the Propagation Constants of a Buried Insulated Conductor", 1970, Air Force Weapons Laboratory EMP Interaction Note No. 50, vol. 4

4. Sunde, E. D., EARTH CONDUCTION EFFECTS IN TRANSMISSION SYSTEMS, Dover, N. Y., 1968

5. Ramo, S., Whinnery, J. R., FIELDS AND WAVES IN MODERN RADIO, John Wiley and Sons, Inc., N.Y., 1953 (second edition)

6. Jordan, E. C., Balmain, K. G., ELECTROMAGNETIC WAVES AND RADIATING SYSTEMS, Prentice-Hall, Inc., New Jersey, 1968 (second edition)

7. Stratton, J. A., ELECTROMAGNETIC THEORY, McGraw-Hill Book Co., Inc., N.Y., 1941

8. Abramowitz, M., Stegun, I. A., HANDBOOK OF MATHEMATICAL FUNCTIONS, Dover, N. Y., 1964

9. Sommerfeld, A., Ann. d. Physik 67, 233 (1899)

10. Feynman, R. P., Leighton, R. B., Sands, M., THE FEYNMAN LECTURES ON PHYSICS, Addison-Wesley Publishing Company, N. Y., Vol. II, 1963

APPENDIX C

COMPARISON OF A BARE WIRE SURFACE CABLE ESTIMATE

AND RESULTS FROM A GREENS FUNCTION TREATMENT

OF A WIRE NEAR A FINITELY CONDUCTING GROUND PLANE

Here we compare the two cable models (infinite bare wires, uniform overhead illumination) shown below in Figure C-1.

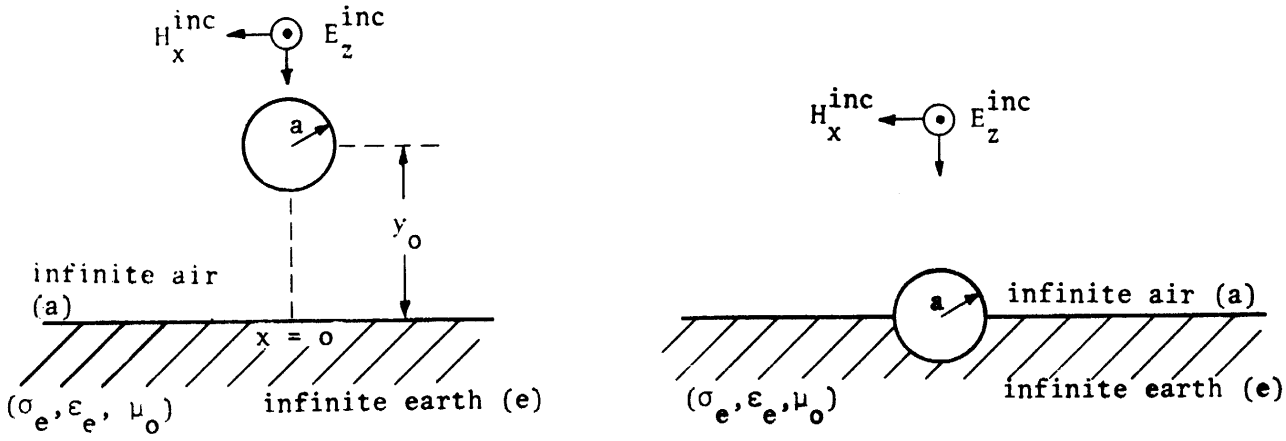

a) wire near ground, but with $y_o >> a$

b) surface cable; treatment analogous to that of reference 1

Figure C-1.

Bombardt [5] has solved by Greens function techniques a more general version of problem C-1 (a) (oblique incidence, axis of wire at $x > 0$). An application of L'Hospitals rule to the current equation in [5]

and analytic evaluation of all but one integral yields the Bombardt result for the total wire current in the limiting geometry of Figure C-1(a):

$$I(\omega) = \frac{4E_z^{inc}(\omega)e^{-ik_a y_o}\left[1 + \left(\frac{k_a - k_e}{k_a + k_e}\right)e^{2ik_a y_o}\right]}{\mu_o \omega \left[H_o^{(1)}(k_a a) + H_o^{(1)}(2k_a y_o)\,\overline{F}\right]} , \tag{1}$$

where,

$$\overline{F} = \frac{2e^{ik_a y_o}(1 - ik_a y_o) - \pi y_o^2 (I_A + I_B)}{2e^{ik_a y_o}(1 - ik_a y_o) + \pi y_o^2 (I_A + I_B)} \tag{2}$$

and,

$$I_A = \frac{2k_a^2}{\pi}\int_o^1 \left[\frac{k_e^2}{k_a^2} - 1 + u^2\right]^{1/2} e^{ik_a y_o u} du , \tag{4}$$

$$I_B = \frac{(k_a^2 - k_e^2)^{1/2}}{y_o}\left[H_1[y_o(k_a^2 - k_e^2)^{1/2}] - Y_1[y_o(k_a^2 - k_e^2)^{1/2}]\right] . \tag{5}$$

The function H_1 in (5) denotes the order one Struve function. Integral (4) is easily done numerically.

For the surface cable in C-1(b) we use the "average" approximation from [1] for the effective impedance:

$$Z_{s.cable} = \frac{2Z(k_a)Z(k_e)}{Z(k_a) + Z(k_e)} , \tag{6}$$

where,

$$Z(k) = \frac{-i\mu_o \omega H_o^{(1)}(ka)}{2\pi k a H_1^{(1)}(ka)} . \tag{7}$$

The impedance (7) is a familiar textbook result. The incident field is multiplied by the overhead transfer function as in the previous section 3 calculations. Interface effects are, of course, "built in" to the Bombardt result (1).

Assuming the same incident pulse shape as in section 3, a comparison of results is shown in Figure C-2. The surface cable model yields a good estimate of the current induced on a (electrically thin) wire near (≤ 1 m) the earth's surface. The Bombardt result is insensitive to y_o for $y_o \leq 1$ m and in both cases we have $y_o a$ reasonably large as required in the derivations of [5]. Had we employed simply $Z(k_e)$ rather than (6) for the surface cable impedance, the resulting current estimate would be only ~15% larger.
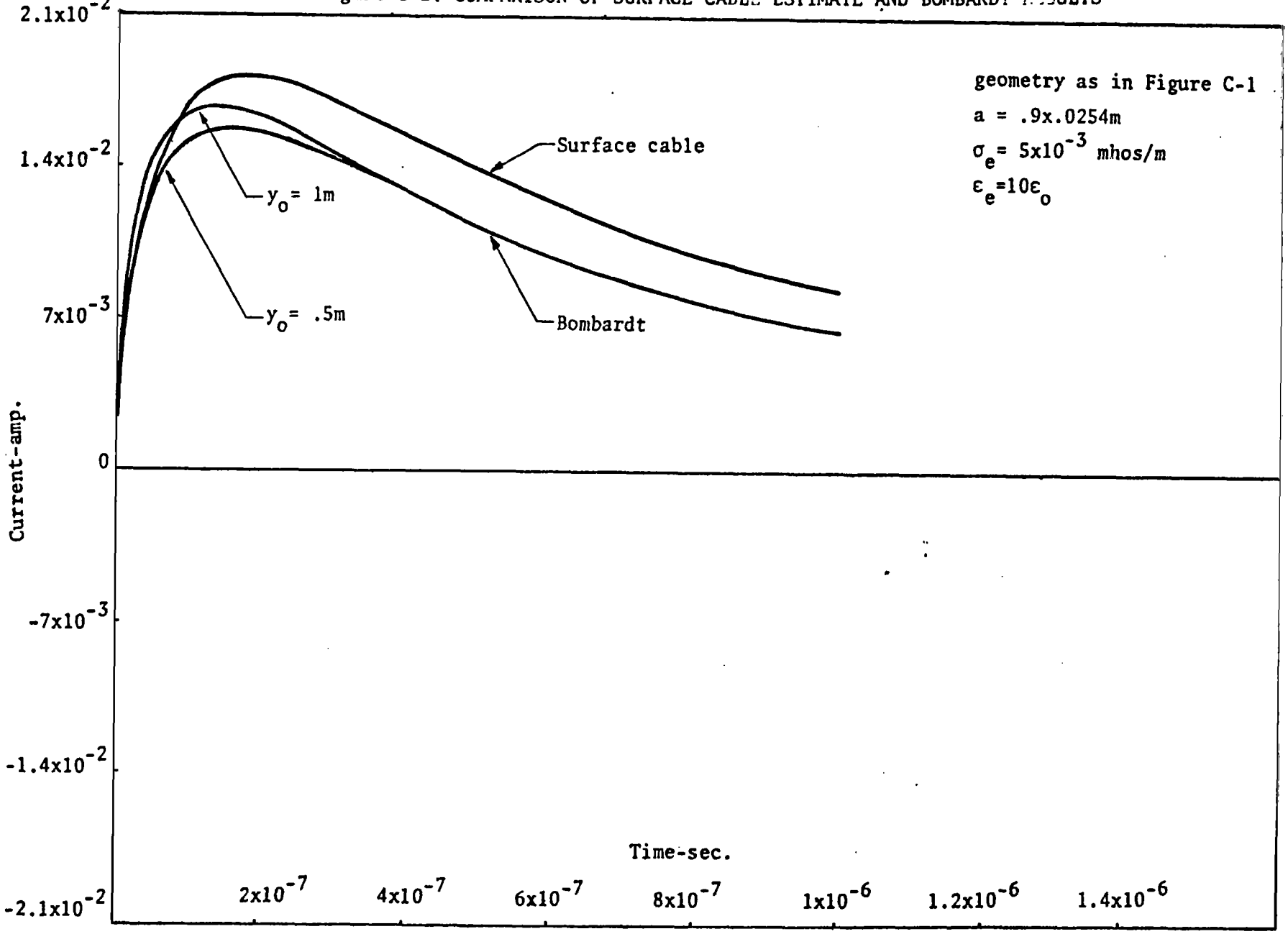
Figure C-2: COMPARISON OF SURFACE CABLE ESTIMATE AND BOMBARDT RESULTS